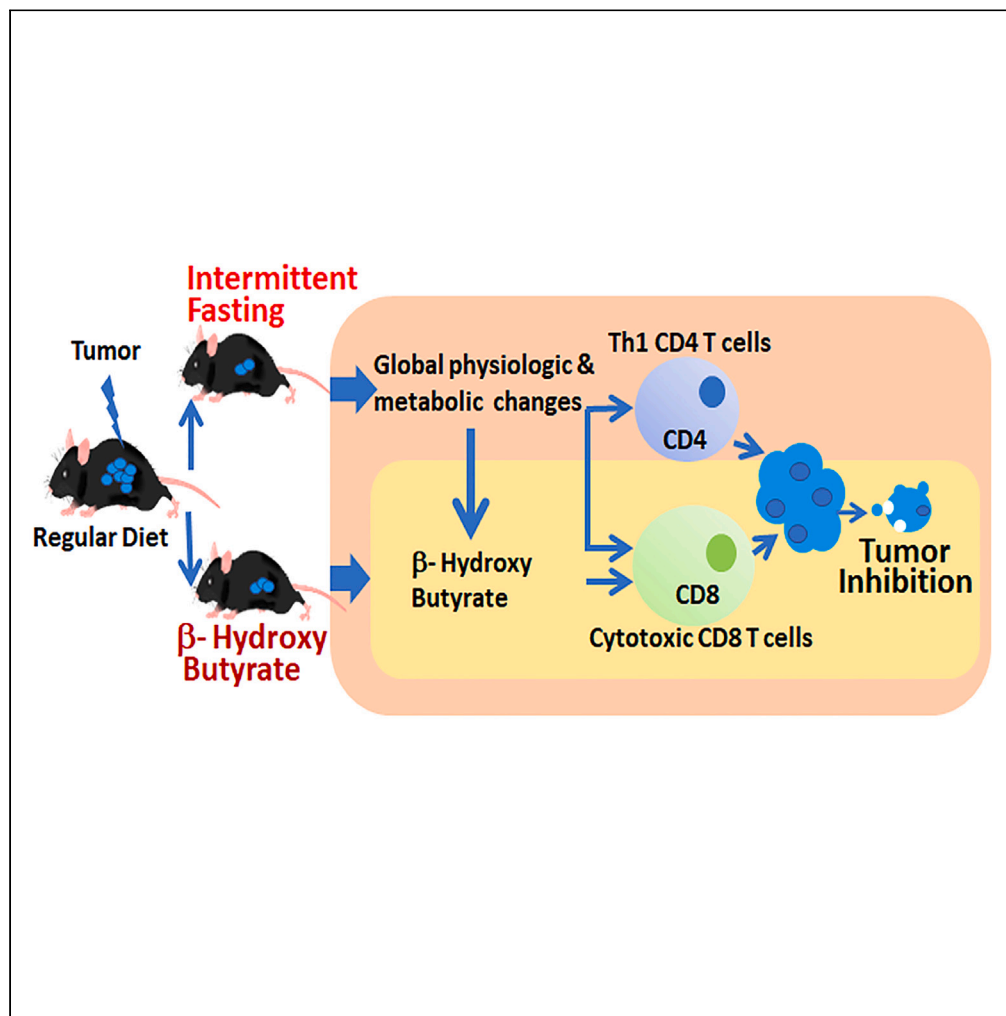


Article

Intermittent fasting induced ketogenesis inhibits mouse epithelial ovarian cancer by promoting antitumor T cell response



Mary Priyanka Udumula, Harshit Singh, Faraz Rashid, ..., Adnan Munkarah, Shailendra Giri, Ramandeep Rattan

rrattan1@hfh.s.org

Highlights

IF increases survival and potentiates T cell-mediated immune responses in EOC

IF-mediated protective effects were abolished in the absence of T cells

IF resulted in abundance of BHB, which recapitulated the anti-tumor effects of IF

IF improved survival more than exogenous BHB therapy

Udumula et al., iScience 26, 107839
October 20, 2023 © 2023 The Author(s).
<https://doi.org/10.1016/j.isci.2023.107839>

Article

Intermittent fasting induced ketogenesis inhibits mouse epithelial ovarian cancer by promoting antitumor T cell response

Mary Priyanka Udumula,¹ Harshit Singh,¹ Faraz Rashid,² Laila Poisson,³ Nivedita Tiwari,¹ Irina Dimitrova,¹ Miriana Hijaz,¹ Radhika Gogoi,⁴ Margaret Swenor,⁵ Adnan Munkarah,¹ Shailendra Giri,² and Ramandeep Rattan^{1,6,7,8,*}

SUMMARY

In various cancer models, dietary interventions have been shown to inhibit tumor growth, improve anti-cancer drug efficacy, and enhance immunity, but no such evidence exists for epithelial ovarian cancer (EOC), the most lethal gynecologic cancer. The anticancer immune responses induced by 16-h intermittent fasting (IF) were studied in mice with EOC. IF consistently reduced metabolic growth factors and cytokines that stimulate tumor growth, creating a tumor-hostile environment. Immune profiling showed that IF dramatically alters anti-cancer immunity by increasing CD4⁺ and CD8⁺ cells, Th1 and cytotoxic responses, and metabolic fitness. β -hydroxy butyrate (BHB), a bioactive metabolite produced by IF, partially imitates its anticancer effects by inducing CD8⁺ effector function. In a direct comparison, IF outperformed exogenous BHB treatment in survival and anti-tumor immune response, probably due to increased ketogenesis. Thus, IF and one of its metabolic mediators BHB suppress EOC growth and sustain a potent anti-tumor T cell response.

INTRODUCTION

Epithelial ovarian cancer (EOC), the most prevalent form of ovarian cancer, is the primary cause of mortality due to gynecologic cancer in the US. Despite breakthroughs in therapy choices for EOC, its prognosis remains dismal, with a survival rate that has remained unchanged for decades at 45%, and approximately 20% for those diagnosed at a late stage, making it the fifth leading cause of cancer-related death in women.¹ The multimodal treatment for EOC consists of maximal surgical resection followed by chemotherapy with platinum and taxanes. The recent introduction of PARP inhibitors and anti-angiogenic treatments has provided some advantages. Despite the fact that the majority of patients initially respond to the treatments, more than 80% will recur within two years, limiting the benefits of treatment. In addition, the financial toxicity associated with chemotherapy is an added burden for EOC patients, diminishing their quality of life (QoL).^{2,3} Consequently, it is of the utmost importance to identify complementary approaches that can improve therapy efficacy while causing minimal toxicity. An understudied and undervalued area in EOC is the modulation of environmental factors that play a key role in determining the balance between disease and outcome. Among the numerous environmental influences, nutrition has been demonstrated to influence disease development, therapeutic response, and survival in a variety of cancers,^{4,5} but such evidence is scarce in EOC. In addition, there are currently no universally accepted dietary recommendations for EOC patients that might improve their prognosis and survival.

Dietary restriction is one of the oldest diet-based interventions applied and tested in cancer and other disorders.^{6,7} It has been demonstrated that caloric restriction reduces the risk of several metabolic illnesses, enhances life expectancy, and inhibits cancer growth.^{8,9} Recent studies have indicated that the ketogenic diet, which severely restricts carbohydrates and causes ketosis, can improve the prognosis of numerous diseases and cancer.^{10–12} Fasting is another approach to achieve ketosis, with intermittent fasting (IF) being the most popular, extensively used, and scientifically proven to confer similar health benefits, particularly on cancer growth.¹³ IF can induce metabolic responses and adaptations that can have far-reaching effects on a patient's physiology, including the rate of tumor progression, treatment response, anti-tumor immune response, and QoL.^{7,13–15} While long-term fasting schedules have not been examined in cancer patients, a small number

¹Department of Women's Health Services, Henry Ford Hospital and Henry Ford Cancer Institute, Detroit, MI, USA

²Metabolomics Core, Department of Neurology, Henry Ford Hospital, Detroit, MI 48202, USA

³Department of Public Health Services and Center for Bioinformatics and Henry Ford Cancer Institute, Detroit, MI, USA

⁴Department of Gynecology Oncology, Barbara Ann Karmanos Cancer Institute and Wayne State University, Detroit, MI, USA

⁵Department of Lifestyle and Functional Medicine, Henry Ford Hospital and Henry Ford Cancer Institute, Detroit, MI, USA

⁶Department of Oncology, Wayne State University, Detroit, MI, USA

⁷Department of Ob/Gyn, Michigan State University, East Lansing, MI, USA

⁸Lead contact

*Correspondence: rrattan1@hfhs.org

<https://doi.org/10.1016/j.isci.2023.107839>



of clinical trials have shown the combination of short-term fasting (24–72 h fast) with chemotherapy, to be feasible, safe and result in reduced chemotherapy side effects and better QoL measures.^{16–18}

Recent recognition of reprogramming of immunometabolism as a crucial event regulating the function of all immune cells has pushed research into dietary interventions that influence the immune system. Recent cancer studies have eloquently demonstrated the ability of ketogenic and other restrictive diets to stimulate an efficient anti-tumor immune response.^{11,19,20} None of these investigations, however, have been conducted in EOC. Here, we assessed the effect of a 16-h fast and 8-h feeding IF on survival and immune response against the tumor in preclinical models of syngeneic EOC. We found that IF increases overall survival via enhancing T cell antitumor immunity, and via buildup of the ketone body BHB (β -hydroxy butyrate), regardless of the tumor's mutational signature. Our research demonstrates the efficacy of IF as an adjuvant intervention and a strategy to improve antitumor immune response in EOC.

RESULTS

If improves overall survival in EOC mouse models irrespective of mutational markers

We compared the anti-tumor effects of a 16-h IF intervention to those of a non-fasting regular diet (RD) control group in C57/B6 mice. RD and IF mice were injected intraperitoneally (IP) with syngeneic ID8 ovarian tumor cells (ID8^{p53+/+} or ID8^{p53-/-} or ID8^{p53-/-, PTEN-/-}), a widely used transplantable murine model to generate peritoneal ovarian tumors.^{21,22} Survival was significantly improved by 27 days in IF mice with ID8^{p53+/+} tumors (median survival 86.5 days) compared to RD (median survival 69 days) (Figure 1A). The improved survival was accompanied by a relative stabilized weight trend in the IF mice, as opposed to the RD mice, whose weights increased (Figure 1B). The IF mice had a smaller abdominal circumference as a surrogate for ascites burden (Figure 1C) and a smaller volume of accumulated ascites (Figure 1D) than the RD mice. Mice with ID8^{p53-/-} tumors, indicative of the aggressive high-grade serous ovarian cancer,^{22,23} exhibited an improvement of 19 days when subjected to IF (median survival 70 days) compared to mice with RD tumors (median survival 51 days) (Figure 1E). Similarly, the IF mice exhibited a stable weight pattern, decreased abdominal circumference and ascites volume (Figures 1F–1H). Mice with ID8^{p53-/-, PTEN-/-} tumors, which are indicative of enhanced aggressiveness,²² showed an improvement of 20 days when subjected to IF (median survival 58 days vs. 38 days in the RD group) (Figure 1I). Likewise, the IF mice exhibited a stable weight trend, decreased abdominal circumference, and decreased ascites volume (Figures 1J–1L). To determine the visual impact on tumors, we implanted subcutaneous ID8^{p53-/-} tumors and subjected a subset of mice to IF. In the control group, tumors were measurable beginning on day 35, but tumors in the IF group did not become measurable until about 42 days and grew more slowly as represented by the ultimate tumor size and tumor wet weight at endpoint (Figures 1M–1P). Food intake measurements revealed that mice treated to IF ingested nearly the same quantity of food in the 8-h feeding window that the control RD animals ingested daily when fed *ad libitum* (Figures S1A–S1C). In addition, albumin levels assessed after 4–5 weeks of continuous IF and used as a starvation marker²⁴ were comparable between the IF and RD groups (Figures S1D–S1F).

In agreement with previously published findings on other tumor models,^{25,26} we demonstrate for the first time that IF intervention prolongs survival and slows the growth of tumors in syngeneic models of EOC.

If decreases tumor promoting growth and inflammatory factors in EOC mouse models

Dietary restrictions have been associated to a reduction in systemic pro-tumor and inflammatory factors.^{27,28} To evaluate the effect of IF on the tumor microenvironment, an adipokine array was performed on the ascites of RD and IF mice with ID8^{p53-/-} tumors (Figure S2). IF decreased tumor-promoting metabolic growth factors such as IGF-1 and leptin, as well as major pro-tumor and inflammatory factors such as FGF acidic, VEGF, ANGPT, MCP-1, M-CSF, and lipocalin, whereas adiponectin levels rose (Figure S2). Validation by ELISA in the ascites and plasma of RD and IF mice, revealed a reduction in growth factors including IGF-1 (Figures 2A and 2M), insulin (Figures 2B and 2N) and leptin (Figures 2C and 2O) and an increase in adiponectin (Figures 2D and 2P) by IF. Estimation of pro- and anti-inflammatory markers in ascites and plasma revealed that IFN γ , one of the essential cytokines for the cytotoxic CD8⁺ T cells was elevated in the ascites from IF mice compared to RD mice (Figure 2E), but plasma levels remained relatively unaltered (Figure 2Q). Another important anti-inflammatory cytokine IL-10 was also reduced in the ascites and plasma (Figures 2F and 2U) while other pro-inflammatory cytokines including TNF α , IL-6, IL-4, IL-1 β , MCP-1 and GM-CSF were significantly lowered in the ascites and plasma of IF mice (Figures 2G–2L, and 2S–2X). Similar differential regulation by IF was also observed in the ascites and plasma of mice with ID8^{p53-/-, PTEN-/-} tumors (Figure S3).

Thus, IF can differently modify and establish an anti-inflammatory and anti-growth milieu at both the tumor and systemic levels.

If remodels the antitumor T cell immune response to EOC mouse tumors

Recent research has shown that short-term fasting or fasting mimicking diets can modify the immune response in a variety of disease models,^{29,30} but there are no reports in EOC. Immune profiling followed by tSNE projection was done in the tumor environment reflected by ascites and systemically reflected by blood obtained from ID8^{p53-/-} and ID8^{p53-/-, PTEN-/-} tumor carrying mice on IF and RD. The ascites of IF mice showed an increase in number of CD4⁺ and CD8⁺ T cells compared to RD mice (Figures 3A–3D, 3H, and S4). Analysis of the effector markers revealed that CD4⁺ T cells from IF mice displayed a robust Th1 phenotype, as evidenced by elevated intracellular IFN γ and decreased IL-4 expression in ascites (Figures 3B, 3C, and 3E–3G; Figure S4). In contrast to RD mice, the effector, and cytotoxic markers of CD8⁺ T cell were significantly enhanced by IF as seen by increased intracellular production of IFN γ , granzyme B and perforin, (Figures 3B, 3C, and 3I–3K; Figure S4). This was reflected in the CD4⁺ and CD8⁺ T cell profiles in the tumors (Figures 3L–3R) from the subcutaneous model. A similar pattern

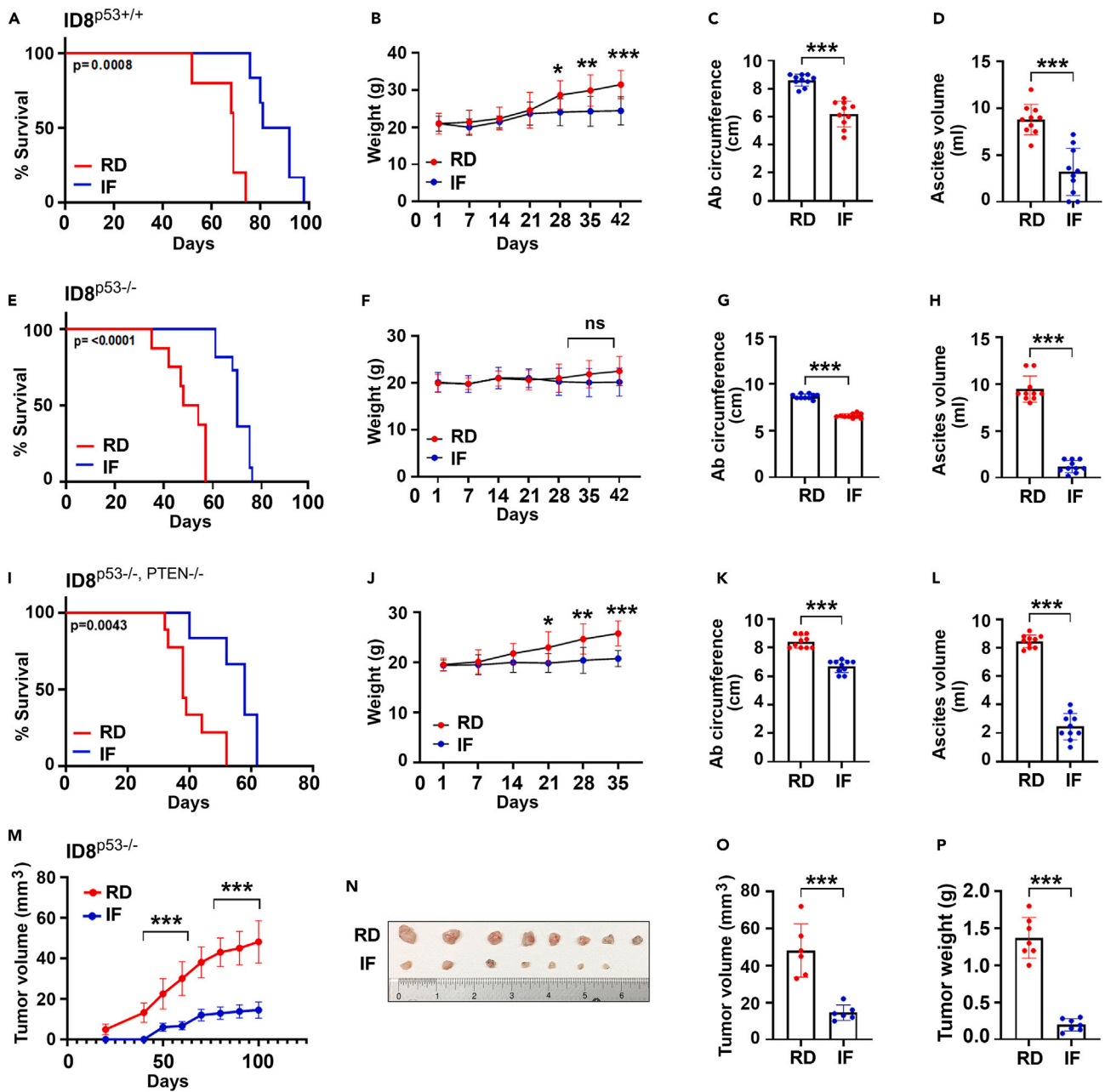


Figure 1. IF improves overall survival in EOC mouse models irrespective of mutational markers

Kaplan-Meier graphs indicating overall survival in mice bearing (A–L) (A) ID8p53^{+/+} EOC subjected to RD or IF (n = 12/group), p = 0.0008 by Gehan-Breslow-Wilcoxon test; (E) ID8p53^{-/-} EOC subjected to RD or IF (n = 12/group), p < 0.0001 by Gehan-Breslow-Wilcoxon test and (I) ID8p53^{-/-},PTEN^{-/-} EOC subjected to RD or IF (n = 12/group), p = 0.0043 by Gehan-Breslow-Wilcoxon test. Average weekly body weight progression in (B) ID8p53^{+/+}, (F) ID8p53^{-/-} and (J) ID8p53^{-/-}, PTEN^{-/-} EOC bearing mice. (C, G, K) Bar graph represents average abdominal circumference at 6 weeks of ID8p53^{+/+}, and at 5 weeks of ID8p53^{-/-} and ID8p53^{-/-}, PTEN^{-/-} EOC bearing. (D, H, and L) Ascites volume collected at 6 weeks from ID8p53^{+/+}, and at 5 weeks from ID8p53^{-/-} and ID8p53^{-/-}, PTEN^{-/-} EOC bearing mice respectively in response to IF. (M) ID8p53^{-/-} subcutaneous tumors growth (n = 8/group). (N–P) (N) Photograph of dissected tumors, (O) Bar graph represents tumor volume at endpoint and, (P) wet tumor weights. **p < 0.01, ***p < 0.001, IF compared with RD group by Student's t test.

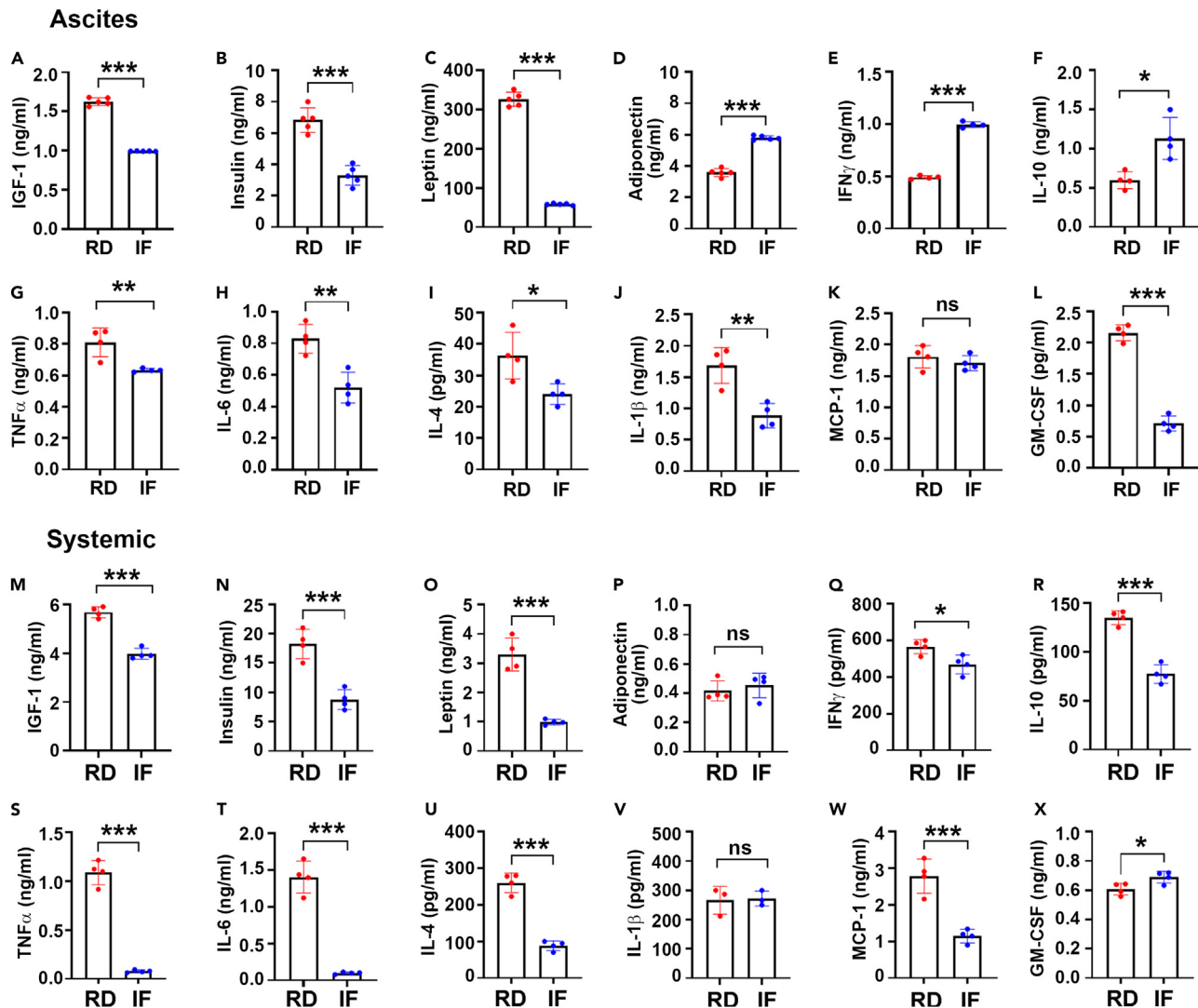


Figure 2. IF decreases tumor promoting growth and proinflammatory factors in EOC mouse models

(A–X) Measurement of (A, M) IGF-1, (B, N) Insulin, (C, O) Leptin, (D, P) Adiponectin, (E, Q) IFN γ , (F, R) IL-10, (G, S) TNF α , (H, T) IL-6, (I, U) IL-4, (J, V) IL-1 β , (K, W) MCP-1 and (L, X) GMCSF in ascites and plasma collected at week 5 from ID8^{p53-/-} EOC bearing mice by ELISA (n = 4 or n = 3). *p < 0.05, **p < 0.01, ***p < 0.001, IF compared with RD group by Student's t test.

was observed in the blood and spleen with significant anti-tumor CD4 and CD8 T cell responses (Figure S5). ID8^{p53-/-}, PTEN^{-/-} tumor mice also showed similar significant anti-tumor CD4 and CD8 T cell responses (Figure S5). Thus, in preclinical models of EOC, our studies indicate that IF can stimulate an anti-tumor T cell response, which may lead to decreased tumor progression and enhanced survival.

Function, differentiation, and activation of T cells are substantially regulated by metabolic modifications.^{31,32} Deprivation of glucose suppresses tumoricidal function of T cells in tumors.³³ In studies such as chronic lymphocytic leukemia, patients have displayed impaired mitochondrial fitness in CD8⁺T cells which led to delay in CAR-T cell efficiency.^{34,35} However, modulation of T cell metabolism by IF is unknown. Compared to RD mice, splenic CD4⁺ cells from IF mice engaged in enhanced glycolysis, as evaluated by ECAR, and decreased OXPHOS, as measured by OCR,³⁶ determined by real-time bioenergetic profiling (Figures 3S and 3T). Interestingly, splenic CD8⁺ T cells from IF mice were more active in both glycolysis and OXPHOS than CD8⁺ cells from RD mice (Figures 3U and 3V). Consequently, CD4⁺ and CD8⁺ cells are metabolically more active in response to IF, which may facilitate their anti-tumor immune function.

Overall, IF can modulate the metabolism of CD4⁺ and CD8⁺ T cells, positioning them to execute their anti-tumor immune response.

The absence of T cells reverses the anticancer effect of IF in EOC mouse tumors

To assess the importance of T cells in IF's anti-tumor impact against EOC, we examined IF in nude mice devoid of thymus and with non-functional T cells.³⁷ Nude mice with ID8^{p53-/-} tumors that have been subjected to IF exhibited no change in survival compared to mice

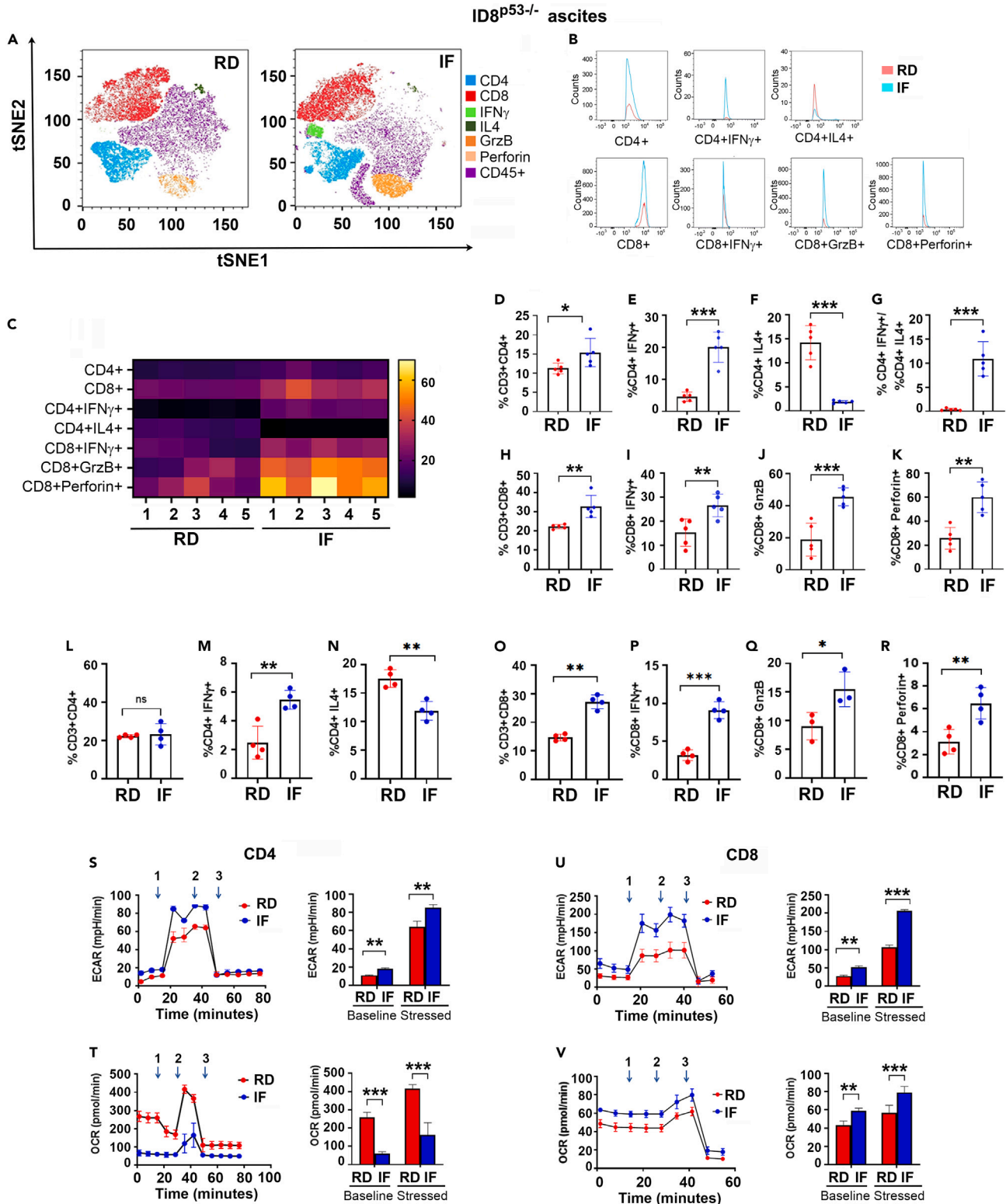


Figure 3. IF remodels the anti-tumor T cell immune response to EOC mouse tumors

(A–R) (A) A representative t-SNE visualization of markers after gating on single, live, CD45⁺ CD3⁺, CD4⁺, CD8⁺, IFN γ , IL4, Granzyme B (Grz B) and perforin expression.

(B) Histograms represent average counts of the main T cell subsets in RD and IF groups.

Figure 3. Continued

(C) Heatmap represents marker expression of the main T cell subsets in individual samples. Bar graph represents the percentage of T cell subsets (D) CD4⁺, (E) CD4+IFN γ +, (F) CD + IL4+, (G) ratio of CD4⁺ IFN γ to CD4+IL4+, (H) CD8⁺, (I) CD8+IFN γ +, (J) CD8+GrzB+ and (K) CD8+perforin+. Immune profiling was performed in 5 individual mice per group. Bar graph represents the percentage of T cell subsets (L) CD4⁺, (M) CD4+IFN γ +, (N) CD + IL4+, (O) CD8⁺, (P) CD8+IFN γ +, (Q) CD8+GrzB+ and (R) CD8+perforin+ in the subcutaneous tumors. Immune profiling was performed in tumors from 4 individual mice per group. (S and U) Extracellular acidification rate (ECAR) in splenic CD4⁺ and CD8⁺ cells (n = 3). (T and V) Oxygen consumption rate (OCR) in splenic CD4⁺ and CD8⁺ cells (n = 3). The experiment was repeated twice in two different sets of mouse experiment. *p < 0.05, **p < 0.01, ***p < 0.001, IF compared to RD group by Student's t test.

on RD (RD median survival of 39 days versus IF median survival of 38 days), body weight, abdominal circumference, or ascites volume (Figures 4A–4D). Measuring metabolic variables revealed that IF decreased IGF-1 while increasing insulin and having no effect on leptin and adiponectin (Figure S6A). Some pro-inflammatory variables, such as IL-4, MCP-1, and GM-CSF, were reduced, while TNF α was elevated, and anti-inflammatory cytokines IFN γ and IL-10 were unaltered (Figure S6B). Thus, while IF can partially alter the TME of EOC in nude mice, it cannot inhibit tumor growth, suggesting a key role for functioning T cells. To further confirm the dependence of IF on T cells in mediating its anticancer effect, we depleted CD4⁺ and CD8⁺ cells in mice undergoing IF (Figures S6C–S6F) and observed that CD8⁺ depletion reversed IF's protective effect, while CD4⁺ depletion was less effective (Figures 4E, S6G). In contrast to CD4⁺ depletion, CD8⁺ depletion reversed the IF mediated increase in survival and decrease in ascites and abdominal circumference (Figures 4F, 4G, S6H, and S6I). These findings imply that T cells are crucial mediators of IF's anti-tumor action, with CD8⁺ cells playing a larger role than CD4⁺ cells.

Use of monoclonal antibodies to block the interaction between programmed cell death protein (PD-1) and its counter ligand programmed death ligand 1 has demonstrated promising therapeutic effectiveness in various malignancies, except in EOC.^{38,39} Since IF improved T cell response, we examined whether it could also improve immunotherapy outcomes. ID8^{P53-/-} injected mice treated with anti-PD 1 in combination with IF exhibited a substantial increase in survival, with a median survival of 93 days compared to 55 days for the RD mice, 70 days for mice on IF alone and 80 days for mice treated with anti-PD1 alone (Figure 4H). Lower abdominal circumference and ascites volume represented the decreased tumor load in the combination group compared to the single therapy and IF groups (Figures 4I and 4J). In the ascites, the anti-tumor CD8⁺ T cell response was enhanced in the combination group, as seen by an increase in the CD8⁺ T cells expressing IFN γ and granzyme B, although IF alone was equally efficient in increasing CD8⁺ cell number and granzyme B expression (Figures 4K–4O). An identical improvement in CD8⁺ T cell response was also detected at the systemic level (Figures S6J–S6N).

These findings demonstrate that T cells are a critical component of IF's anticancer action, and that IF can enhance the anti-tumor CD8⁺ T response induced by PD-1 inhibition.

IF induces ketogenesis

As any dietary intervention would result in central metabolism reconfiguration, we performed untargeted metabolomics on plasma from EOC mice on RD and IF to determine the molecular metabolic mediators of IF (Figure S7A). Principal component analysis^{40,41} demonstrated strong separation along plasma metabolites of RD and IF mice (Figure S7B). The heatmap representation of the significantly 471 altered metabolites revealed clear alterations in all the key super-metabolism pathways (Figure 5A). In response to IF, the MetaboAnalyst Pathway enrichment analysis⁴¹ identified ketone body metabolism as the most significantly enriched pathway (p \leq 0.041, FDR \leq 0.05) (Figures 5B and S7C). Metabolite concentrations of the ketone bodies acetoacetate and BHB were significantly increased (Figures 5C and 5D). In another group of mice, we further validated the increased levels of BHB, the major ketone body generated in the liver and transported to other tissues to be used as fuel,⁴² in plasma and ascites of fasting mice as detected by LC/MS/MS (Figures 5E and 5F) and ELISA (Figures 5G and 5H). Enhanced expression of liver ketogenic enzymes, including ACAT, HMGCS2, HMGCL, and BDH1, correlated with elevated BHB levels (Figures 5I and 5J), indicating enhanced ketogenesis in the liver.

To determine if the bioactive BHB can communicate with and impact T cells, the expression of the BHB receptor, GPR109a,^{43,44} was evaluated on CD4⁺ and CD8⁺ T cells isolated from naive mice and treated with BHB. GPR109a was expressed at a baseline level in both CD4⁺ and CD8⁺ cells, whereas BHB treatment increased GPR109a expression in CD8⁺ T cells, but not in CD4⁺ T cells (Figures 5K and 5L). To further validate, we assessed the BHB uptake by CD4⁺ and CD8⁺ T cells following BHB exposure. Both CD4⁺ and CD8⁺ cells were able to uptake BHB (Figures 5M and 5N), but CD8⁺ cells were able to uptake almost 5 times more BHB than CD4⁺ T cells (Figure 5O).

Overall, IF generated substantial metabolic remodeling at the systemic and cellular levels, with a rise in ketone bodies and metabolism that may have a more profound effect on CD8⁺ T cell activity.

BHB inhibits tumor growth and promotes antitumor CD8⁺ T cell responses in EOC mouse models

To determine if BHB can replicate the anti-tumor and increase T cell response of IF, we administered BHB to mice with ID8^{P53-/-} and ID8^{P53-/-PTEN-/-} tumors. BHB treatment significantly enhanced overall survival in mice with ID8^{P53-/-} tumors (median survival 63 days versus 50 days) and ID8^{P53-/-PTEN-/-} tumors (median survival 70.5 days versus 53.5 days) (Figures 6A and S8A). The body weights of BHB treated mice increased more slowly than those of RD mice, whereas abdominal circumference and ascites volume were significantly reduced in both models (Figures 6B–6D, S8B, and S8C) compared to control. Profiling of the T cell response revealed an unexpected decrease in CD4⁺ T cells, although intracellular IFN γ levels still rose (Figures 6E–6I, S8E, S8G, and S8H). BHB treated ID8^{P53-/-} mice

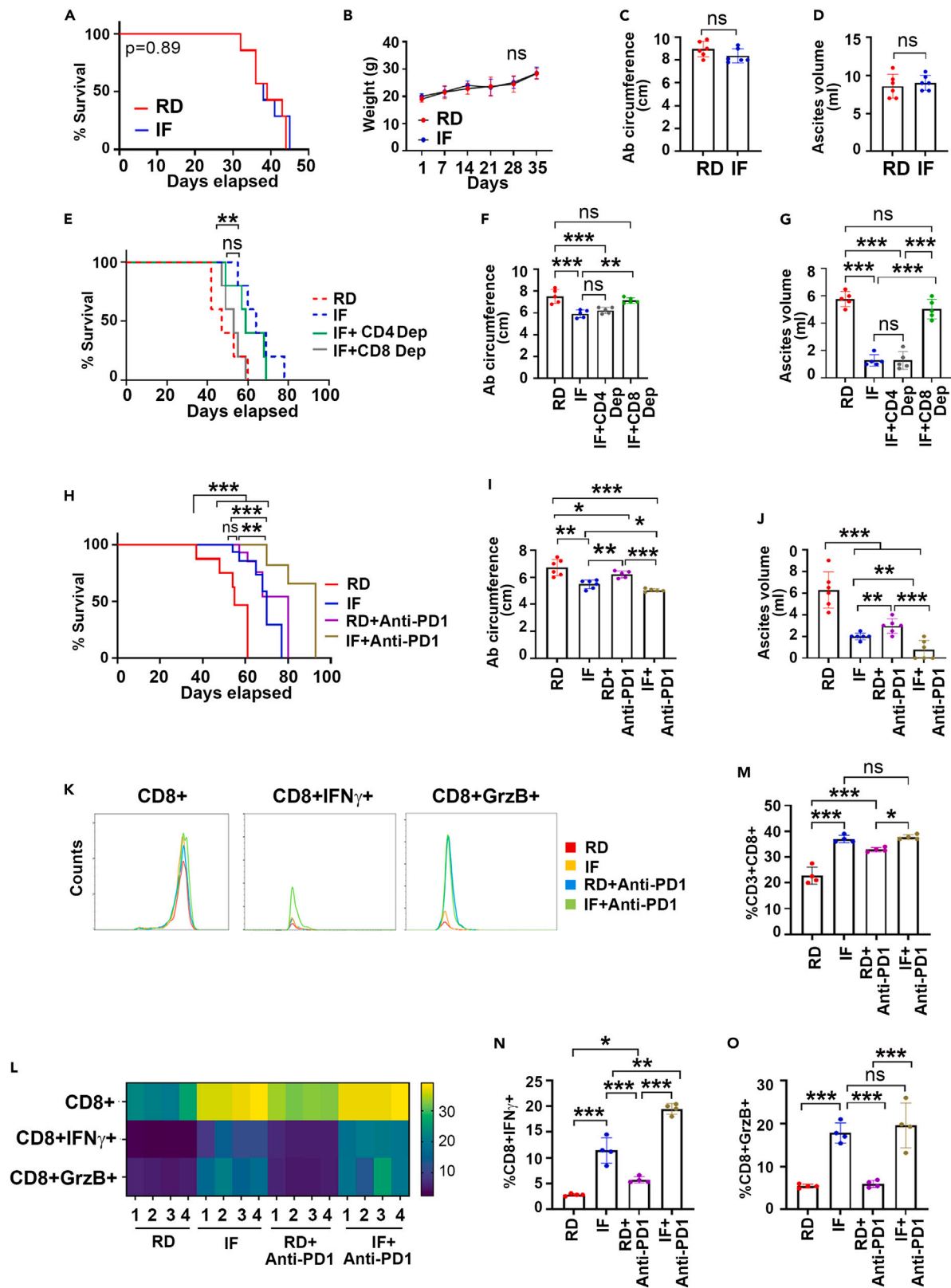


Figure 4. The absence of T cells reverses the anti-cancer effect of IF in EOC mouse tumors

- (A) Kaplan–Meier graph indicating overall survival (n = 12), p = 0.89 by Gehan-Breslow-Wilcoxon test.
 (B) Average weekly body weight progression (n = 12).
 (C) Average abdominal circumference.
 (D) Average ascites accumulated in RD and IF groups.
 (E) Kaplan–Meier graph indicating overall survival mice with CD4⁺ and CD8⁺ depletion (n = 12), p = 0.38 IF compared to CD4 depletion, p = 0.009 IF compared to CD8 by Gehan-Breslow-Wilcoxon test.
 (F) Average ascites accumulated.
 (G) Average abdominal circumference. Data with all control groups is shown in [Figure S6](#).
 (H) Kaplan–Meier graph indicating overall survival in mice with IF and anti-PD1 treatments (n = 12). p = 0.006, IF compared to RD, p = 0.0026 IF compared to IF and anti-PD1 combination, p = 0.0006, RD compared to RD and anti-PD1 combination and p < 0.0001 RD compared to IF and anti-PD1 combination by Gehan-Breslow-Wilcoxon test.
 (I) Average abdominal circumference.
 (J) Average ascites accumulated.
 (K) Histograms representing average CD8⁺, CD8+IFN γ + and CD8+GrzB + abundance at week 5.
 (L) Heatmap representing individual frequency CD8⁺, CD8+IFN γ + and CD8+GrzB + cells.
 (M–O) Percentages of (M) CD8⁺, (N) CD8+IFN γ + and (O) CD8+GrzB+ in RD, IF, anti-PD1 and IF combined with anti-PD1 treated mice. Immune profiling was performed in 4 individual mice per group. *p < 0.05, **p < 0.01, ***p < 0.001, by one-way ANOVA, followed by Sidak multiple comparison test.

exhibited an increase in IL-4 that resulted in a non-significant Th1 response of CD4⁺ cells ([Figures 6J and 6K](#)), but BHB suppressed IL4 production in the ID8^{p53-/-PTEN-/-} mice ([Figure S8I](#)). BHB induced a robust increase in CD8⁺ T cell number and effector markers IFN γ and Granzyme B ([Figures 6E–6G, 6L–6N, and S8I–S8K](#)), as well an increase in CD8:CD4 ratio ([Figure 6O](#)). In the blood of both models, a comparable systemic profile of increased T cell response was also seen in response to BHB ([Figures S9, S8L–S8Q](#), data shown for ID8^{p53-/-}).

Bioenergetic profiling of CD4⁺ and CD8⁺ cells from the spleens of control and BHB treated mice revealed a significant increase in glycolysis measured as ECAR and OXPHOS measured as OCR^{36,41,45} of CD8⁺ T cells alone ([Figures 6R and 6S](#)), but CD4⁺ bioenergetics were relatively unaffected, with increase in OCR alone ([Figures 6P and 6Q](#)). Activated splenic CD8⁺ and CD4⁺ cells were co-cultured with 7AAD labeled ID8^{p53-/-} tumor cells in absence or presence of BHB to confirm that the increased effector expression and metabolic capabilities translated to an increase in function. BHB treated CD8⁺ cells caused more tumor cell death than untreated CD8⁺ cells ([Figures 6T and 6U](#)). Intriguingly, BHB treated CD8⁺ also demonstrated increased proliferation and IFN γ levels ([Figures 6V and 6W](#)), indicating enhanced antitumor capability. In contrast, BHB treated CD4⁺ were unable to induce tumor cell death, despite enhanced proliferation and a non-significant increase in IFN γ levels ([Figures S9J–S9M](#)).

Thus, BHB is an essential modulator of the anti-tumor CD8⁺ response observed during IF in EOC preclinical models.

IF improves EOC survival and antitumor immune response better than BHB

We directly compared the outcomes of IF and BHB in the ID8^{p53-/-} model due to the observation that IF appears to impact both CD4⁺ and CD8⁺ cells, as well as the central metabolism. While BHB treatment enhanced survival compared to untreated control mice on RD, the IF group showed a greater gain in survival (RD median survival 41 days versus 56 days in BHB versus 65 days in IF) ([Figure 7A](#)). Weight changes were comparable across BHB treatment and IF ([Figure 7B](#)). IF mice exhibited lower abdominal circumference and lower ascites volume than BHB mice ([Figures 7C and 7D](#)). Similar decreases in insulin, IGF-1, and leptin levels were observed in both groups, although adiponectin levels were unaffected by BHB in the ascites ([Figure 7E](#)). Both raised the anti-inflammatory IFN γ , although the increase in IF mice was greater ([Figure 7F](#)). All other pro-inflammatory cytokines including TNF α , IL-6, MCP-1 and GM-CSF were reduced in both BHB and IF, although IL-4 and IL-1 β were unaffected by BHB in the ascites ([Figures 7G–7L](#)). Immune profiling of ascites demonstrated that IF significantly increased CD4⁺ and CD8⁺ cell populations, whereas BHB significantly increased only CD8⁺ cells and a trend toward decrease in CD4⁺ cells as seen before ([Figures 7M–7P, 7S](#)). IF demonstrated Th1 intracellular indicators of increased IFN γ and decreased IL-4 in CD4⁺, whereas BHB had no effect on IL-4 as before ([Figures 7M–7O, 7Q, and 7R](#)). Both IF and BHB increased intracellular IFN γ and GrzB in the CD8⁺ cells, although IF caused a greater proportional rise ([Figures 7T and 7U](#)). At the systemic level, a comparable T cell based immunological response was observed ([Figure S10](#)), with differences in CD4⁺IFN γ ⁺ and CD8⁺Granzyme B⁺ stimulation by BHB.

To determine whether the accumulation of BHB differed between the two approaches, we measured BHB levels in the plasma, ascites and T cells of mice from each group. BHB treatment resulted in greater BHB levels in circulation ([Figure 7V](#)), while, IF resulted in significantly higher BHB levels in the ascitic tumor environment ([Figure 7W](#)). Interestingly, IF produced more BHB in both CD8⁺ and CD4⁺ T cells, in contrast to BHB treatment which resulted in BHB accumulation only in the CD8⁺ T cells ([Figures 7X and 7Y](#)). This was supported by expression of BHB receptor GPR109a, where IF and BHB increased the GPR109a expression in CD8⁺ T cells, while in CD4, only IF increased its expression while BHB had no effect ([Figure 7Z](#)).

These observations indicate that IF and BHB have nearly similar impact on the immune response and inflammatory factors, however, they differ in the accumulation of BHB and the expression of its receptor in CD4⁺ cells. Nonetheless, a role for resetting of the physiologic metabolic alterations or of other immune cells, cannot be ruled out and together may be responsible for the greater anti-cancer activity of IF in preclinical models of EOC.

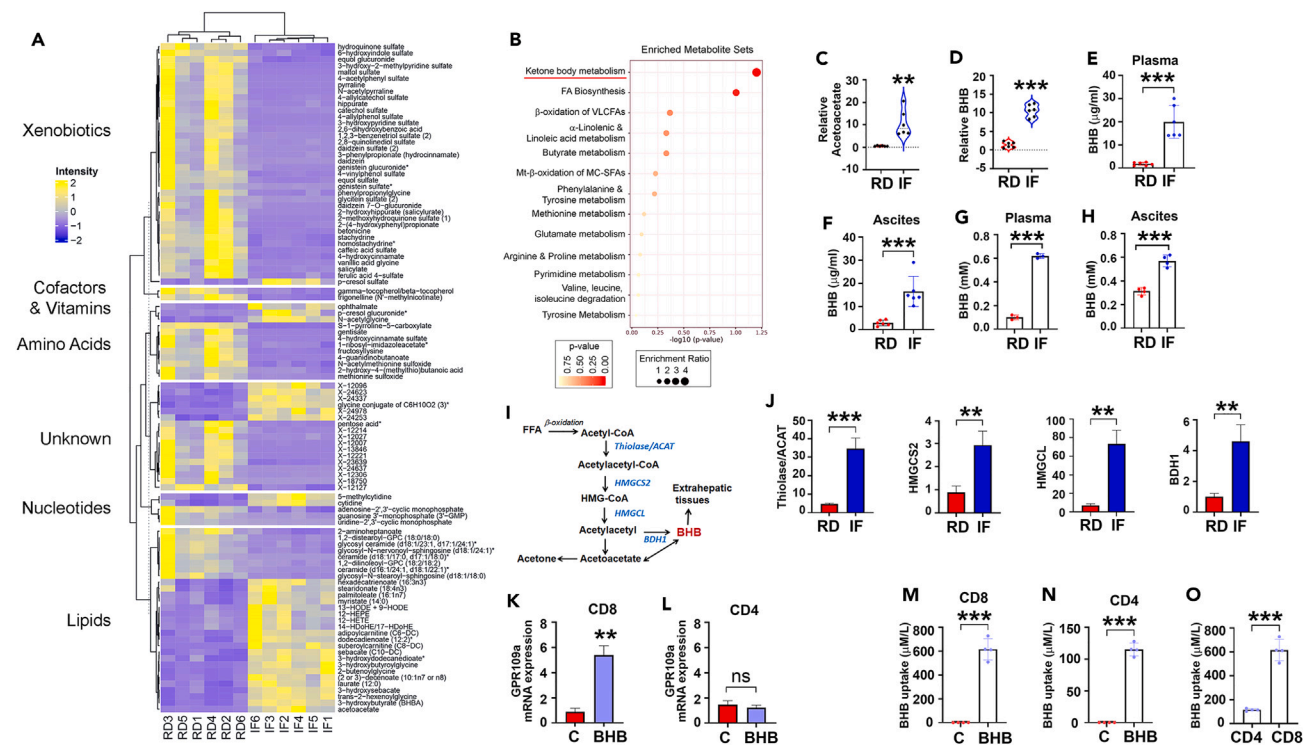


Figure 5. IF induces ketogenesis

(A) Heatmap representation of the significantly altered metabolites in the major super-metabolism pathways in plasma from ID8^{p53-/-} tumor bearing mice (n = 6/group).

(B–D) Pathway enrichment analysis ($p \leq 0.05$; FDR ≤ 0.05). Scaled metabolite intensity graphs showing levels of (C) acetoacetate and (D) BHB.

(E) Plasma BHB levels by LC-MS/MS (n = 6/group).

(F) Ascites BHB levels by LC-MS/MS (n = 6/group).

(G and H) Plasma BHB levels and (H) ascites BHB levels by ELISA (n = 5/group).

(I) Pathway showing enzymes involved in ketogenesis.

(J–N) mRNA expression of liver ketogenic enzymes (J) ACAT, HMGCS2, HMGCL and BDH1 and (K and L) mRNA expression of GPR109a measured by RT-PCR on naive CD8⁺ and CD4⁺ cells respectively in absence or presence of 10mM BHB. BHB uptake measured by LC-MS/MS in naive (M) CD8⁺ cells and (N) CD4⁺ cells after 72 h exposure to BHB.

(O) Ratio of intracellular BHB levels taken up by CD4⁺ and CD8⁺ cells. ** $p < 0.01$, *** $p < 0.001$, IF compared to RD and BHB compared to RD assessed by Student's t-tests.

DISCUSSION

IF is a dietary-based interventional therapy that alternates between fasting and eating over time. The benefits of IF in preventing a variety of diseases and increasing lifespan have prompted interest in its benefits in the field of cancer.¹³ In a number of tumors outside EOC and other gynecologic cancers, numerous studies have examined various IF regimens with varying results. Here, we emphasize IF's capacity to induce anti-tumor immunostimulatory effects via one of its metabolic mediator BHB, which can be leveraged to limit EOC and increase patient survival.

In preclinical models of EOC with increasing aggressiveness,²² the IF regimen comprising of a 16-h fast and an 8-h feeding window for 5 days per week, significantly increased survival. The enhanced survival and decreased tumor growth were associated with an enhanced T cell response against the tumors characterized by a rise in the percentage of CD4⁺ and CD8⁺ cells, an enhancement of their effector function and modulation of their metabolic activity. While it has been shown that a restrictive diet exerts its anti-tumor effects via a decrease in metabolic and growth factors such as IGF-1 and insulin, direct differential stress on tumor cells, nutritional restriction, and reduced inflammation; recent studies have highlighted their immunomodulatory effect.^{7,9} Our work demonstrate that T cells were important for IF-mediated enhanced survival and decreased tumor growth, since nude mice with ovarian cancer gained no benefit from IF. We also found that IF enhanced the efficacy of anti-PD1 immunotherapy in preclinical models of EOC. Studies on T cell depletion reveal that CD8⁺ T cells are more crucial than CD4⁺ T cells in IF-induced anti-tumor T cell response. The correlation between higher effector T cell function and increased metabolic activity of T cells in response to IF suggests that reprogramming of cellular metabolism may be a potential mechanism by which IF regulates the number and function of T cells. Together, our research reveals that IF's immunomodulatory capacity is the primary reason of its anti-tumor activity in preclinical models of EOC.

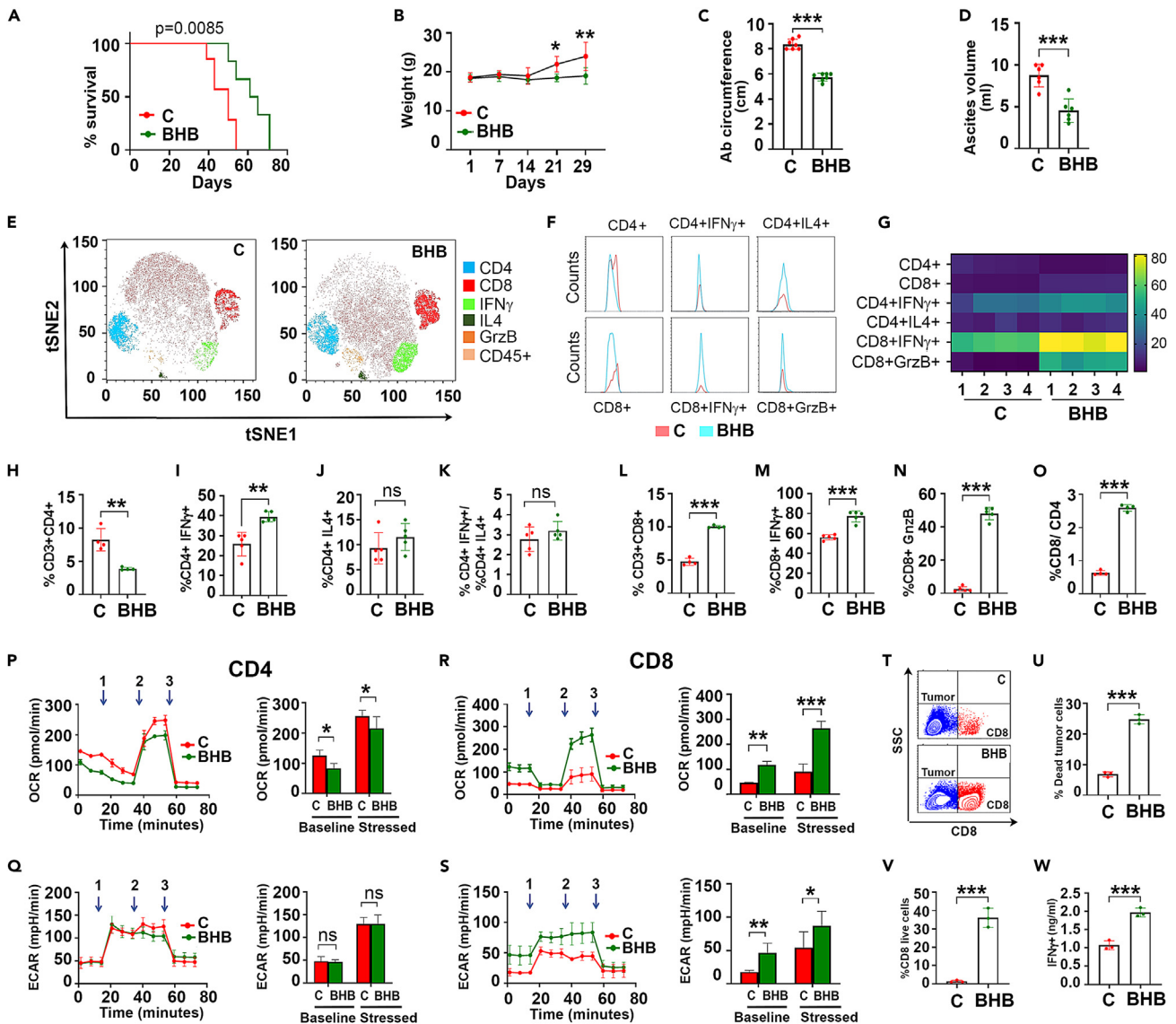


Figure 6. BHB inhibits tumor growth and promotes anti-tumor CD8⁺ T cell responses in EOC mouse models

(A) Kaplan–Meier graph indicating overall survival (n = 12), p = 0.0085 by Gehan-Breslow-Wilcox test.
 (B) Average weekly body weight progression.
 (C) Average abdominal circumference.
 (D) Average ascites volume.
 (E) A representative t-SNE visualization of markers after gating on single, live, CD45⁺ CD3⁺, CD4⁺, CD8⁺, IFN γ +, IL4+ and Granzyme B + (GrzB) cells.
 (F) Histogram represents counts of the T cell.
 (G–O) Heatmap represents marker expression of the T cell subsets. Bar graph represents the percentage of T cell subsets (H) CD4⁺, (I) CD4+IFN γ +, (J) CD + IL4+, (K) ratio of CD4⁺ IFN γ + to CD4+IL4+, (L) CD8⁺, (M) CD8+IFN γ +, (N) CD8+Grz B+ and (O) ratio of CD8⁺ to CD4⁺ cells. Immune profiling was performed in 4 individual mice per group.
 (P and R) Oxygen consumption rate (OCR) in (P) CD4⁺ and (R) CD8⁺ cells (n = 3).
 (Q and S) Extracellular acidification rate (ECAR) in (Q) CD4⁺ cells and (S) CD8⁺ cells (n = 3). The bar graph represents basal and stressed OCR and ECAR. The experiment was repeated twice in two different sets of mouse experiment (n = 3).
 (T–V) percentage of live and dead ID8^{p53-/-} and CD8⁺ cells.
 (W) IFN γ levels (n = 3). *p < 0.05, **p < 0.01, ***p < 0.001, BHB compared to C, assessed by Student's t-tests.

IF or fasting alone has been studied in a variety of malignancies, using different fasting duration and diet type.¹³ The physiologic and metabolic alterations differ based on duration and frequency of fasting, which may determine the outcome and the underlying mechanisms. The antitumor effects of IF have been attributed to weight-loss, creating a tumor environment characterized by decreased growth and metabolic factors, reduced

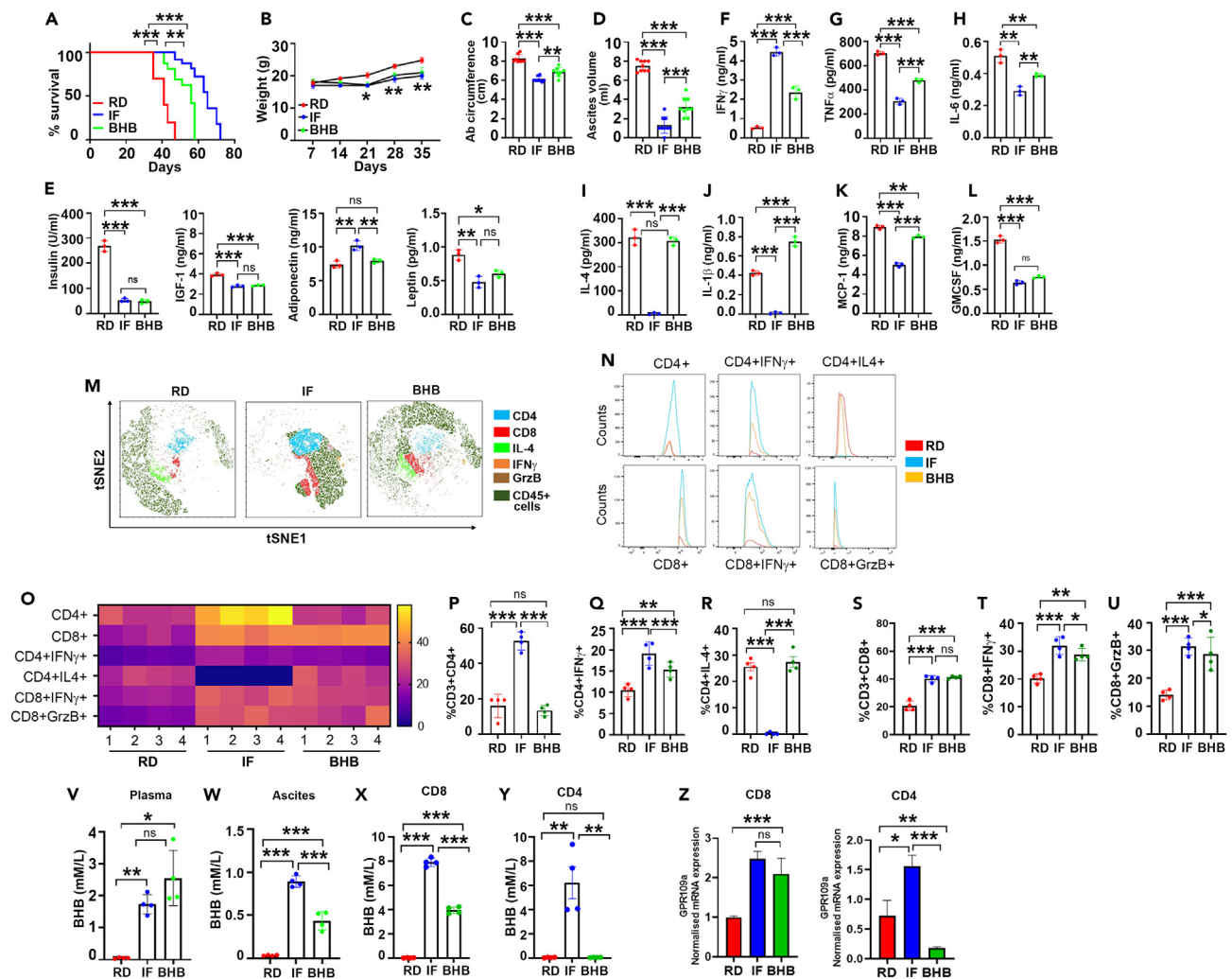


Figure 7. IF improves EOC survival and anti-tumor immune response better than BHB

(A) Kaplan–Meier graph depicting overall survival (n = 12/group), $p < 0.0001$ IF compared to RD, $p < 0.0001$ BHB compared to RD and $p = 0.0016$ BHB compared to IF by Gehan–Breslow–Wilcoxon test.

(B) Average weekly body weight progression.

(C) Average abdominal circumference.

(D–M) (D) Average ascites volume. Growth factors and cytokines were measured in ascites collected at week 5 by ELISA (n = 3/group), (E) Insulin, IGF-1, leptin, and adiponectin, (F) IFN γ , (G) TNF α , (H) IL-6, (I) IL-4, (J) IL-1 β , (K) MCP-1 and (L) GMCSF. (M) A t-SNE visualization of markers after gating on single, live, CD45 $^{+}$ CD3 $^{+}$, CD4 $^{+}$, CD8 $^{+}$, IFN γ^{+} , IL-4 $^{+}$ and Granzyme B+ (GrzB) cells.

(N) Histogram represents average counts of the T cell subsets measured.

(O–U) Heatmap represents marker expression of the measured T cell subsets in individual samples.

(P–Y) Percentages of T cell subsets (P) CD4 $^{+}$, (Q) CD4+IFN γ^{+} , (R) CD4+IL4 $^{+}$, (S) CD8 $^{+}$, (T) CD8+IFN γ^{+} , and (U) CD8+Gnz B+. Immune profiling was performed in 4 individual mice per group. BHB levels measured in (V) plasma, (W) ascites, (X) CD8 $^{+}$ and (Y) CD4 $^{+}$ cells.

(Z) mRNA expression of GPR109a measured by RT-PCR on CD8 $^{+}$ and CD4 $^{+}$ cells isolated from mice on RD, IF or treated with BHB. * $p < 0.05$, ** $p < 0.01$, *** $p < 0.001$, ns = non-significant by one-way ANOVA, followed by Sidak multiple comparison test.

inflammation, and low oxidative stress. Such changes can induce autophagy, apoptosis, and enhance chemotherapy response by differentially protecting normal cells but not the cancer cells. We also found that IF decreased the levels of tumor promoting growth factors and inflammatory cytokines. Although IF has been found to reduce overall inflammation significantly, we observed bidirectional changes in some pro- and anti-inflammatory cytokines. It is difficult to determine the specific consequences of IF on pro and anti-inflammatory cytokines as they are secreted by a variety of immune cells, as well as tumor cells and have differential effect depending on their autocrine and paracrine functions. We postulate that IF creates an equilibrium between anti and pro-inflammatory cytokines that results in an optimal enhanced immune response.

More recently, such dietary interventions have also been shown to promote anti-tumor immune responses.^{7,46} Studies combining various fasting schedules with chemotherapy have demonstrated a significant slowing of tumor progression in preclinical models of many cancer

types.^{15,47} While long-term fasting schedules have not been evaluated in cancer patients, a handful of small clinical trials have evaluated the combination of short-term fasting (24–72 h fast) with chemotherapy, with an emphasis on lowering chemotherapy side effects and enhancing QoL measures.^{16–18} Collectively, these studies demonstrate that fasting in combination with chemotherapy in cancer patients, including ovarian cancer patients, is achievable with a moderate to high adherence rate and results in a substantial enhancement of QoL. Current and future clinical trials are being actively performed and designed to also investigate the mechanisms and effect on cancer cells and patient survival. Thus, IF is a potential promising approach that can be incorporated into patient treatment and management to not only improve QoL, but also successfully inhibit tumor growth, enhance chemotherapy and boost anti-cancer immune response.

Ketone bodies are generated predominantly in the liver by ketogenesis from beta-oxidation of free fatty acids (FFA) and then transported to extrahepatic peripheral organs for oxidation, a process known as ketosis or ketolysis. Under many physiologic situations, including caloric restriction, fasting, starvation, post-exercise, pregnancy, neonatal stage, and low-carbohydrate diets such as the ketogenic diet, ketone body oxidation becomes the primary alternative contributor to energy metabolism in extrahepatic organs, such as muscle, heart, and brain. To determine the metabolic determinant of IF's immunomodulatory function we performed plasma metabolomic profiling. IF triggered dramatic alterations in the central metabolism, including the metabolic switch from glucose to fatty acids and ketone bodies as the primary energy source. This was demonstrated by the enhancement of ketone body metabolism in the plasma of IF-fed mice, the considerable increase in systemic BHB levels, and the enhancement of ketogenesis enzyme expression in the liver. Elevated amounts of BHB were similarly detected in the TME of ascites. BHB is a potent endogenous metabolite that functions as a signaling mediator, epigenetic regulator, protein post-translation modifier, and regulator of inflammation and oxidative stress, in addition to its role as an alternative energy source.^{42,48,49}

With the recent trials of ketogenic diets in cancer, the role of ketosis in cancer biology is still not completely understood; nevertheless, BHB-based research has yielded contradictory results. Studies have suggested that BHB supplementation could inhibit, stimulate, or have no effect on tumor growth.^{12,44,50–55} However, *the effect of BHB in ovarian cancer is largely unknown*. A recent *in vitro* study demonstrated that BHB had no influence on the proliferation or EMT or stem cell characteristics of ovarian cancer cell lines in a low glucose environment, despite an increase in few enzymes of the ketogenesis pathway.⁵⁶ Few recent studies indicate modest benefits of ketogenic diet for ovarian cancer patients.^{57,58} Recent research demonstrates that BHB has an immunomodulatory effect that can enhance the immune response against tumors. By boosting CD8⁺ T cells, BHB has been shown to improve the efficacy of checkpoint-based immunotherapy in melanoma, lung, and renal cell cancer models.¹¹ In healthy human volunteers, BHB has been demonstrated to have a dramatic effect on CD4⁺ and CD8⁺ T response and improve T cell immunity.⁵⁹ Our study indicates that treatment with BHB replicated tumor regression, enhanced survival, modulation of metabolic growth factors and cytokine, and immunomodulatory effects of IF. Interestingly, BHB had a greater immunostimulatory effect on CD8⁺ cells than on CD4⁺ cells, as indicated by substantial increase in CD8⁺ T cell numbers and effector markers IFN γ and granzyme B whereas its effect on CD4⁺ cells was minimal. This differential effect may be explained by the higher expression of the BHB receptor GPR109a,⁴³ and the increased uptake of BHB by CD8⁺ cells compared to CD4⁺ T cells. Compared to CD4⁺ cells, the BHB-treated mice's CD8⁺ cells exhibited significantly higher bioenergetics, as seen by an increase in OCR and ECAR. Functionally, BHB-treated CD8⁺ cells were enhanced in their ability to kill tumor cells, as seen by an increase in CD8⁺ T cells and IFN γ relative to CD4⁺ cells, demonstrating that the anti-tumor effect of BHB is a direct result of its effect on the function and metabolism of CD8⁺ T cells. Overall, BHB appears to be a promising therapeutic agent, which may open new avenues for its application in the treatment and prevention of EOC.

A direct comparison of IF and BHB found that IF is more effective than BHB in slowing tumor progression and prolonging survival. The only significant difference between IF and BHB profiles was the decreased IL-4 and enhanced CD4⁺ activation. A key difference was the accumulation of increased BHB in the CD8⁺ and CD4⁺ T cells of IF mice compared to BHB treated mice and the absence of BHB in CD4⁺ T cells. A plausible explanation could be the ketogenesis mediated intra-cellular production of BHB in case of IF, while in BHB treated mice, BHB accumulation is dependent on its transport via its receptor. Decreased GPR109a expression on CD4⁺ T cells in BHB, would agree with the observations of BHB being ineffective in promoting CD4⁺ function. However, the observation that depletion of CD8⁺ reversed the anti-tumor impact of IF, while CD4⁺ depletion had only a partial effect, suggests a stronger role for the CD8⁺ T cell based immune response in IF too, but one that may require equal activation of CD4⁺ cells to reach its full potential. Recent studies demonstrate the significance of CD4⁺ T cells in the cytotoxic effector activity of CD8⁺ T cells.⁶⁰ It is possible that the greater effect of IF involves other metabolic alterations or another anti-tumor metabolite(s) that directly inhibit tumor-promoting machinery. It is also known that fasting induces widespread changes in the gut microbiome that are disease-alleviating and anti-cancer.⁶¹

Individual metabolic heterogeneity and adherence variability make it difficult to regulate ideal circulation BHB levels with food, which makes the therapeutic application of BHB appealing. However, the contradictory reports show that BHB plays a paradoxical role. Many parameters may be contributing to the diverging effects, such as the nutritional and bioenergetic state of the tumor cells, the right threshold levels of BHB, or the tumor cells' ability to undergo ketolysis, as well as the tumor's type and its location. Those parameters may determine whether BHB is used as a fuel by tumor cells to live and proliferate, is preferentially taken up by immune cells for immunological activation, or influences transcription gene expression as an epigenetic regulator. Therefore, more research is required to investigate BHB as a potential therapeutic agent and to determine the optimal balance between its effects on tumor cells and immune cell activity. On the other hand, findings regarding the anti-tumor effect of IF have been promising, indicating powerful anti-cancer benefits, and no evidence of increasing cancer progression. While we have detailed the immune-enhancing benefits of dietary alterations, there is evidence that dietary modifications also involve metabolic, microbiome, and genetic epigenetic changes, and it may well be the interaction of all these factors that results in tumor suppression.

In conclusion, strategies based on fasting show great promise and our data supports investigating IF in pilot studies of EOC patients. However, there is a clear need to standardize the restriction length and timings as well as to monitor for any long-term negative effects, particularly on immune cells and tumor cells.

Limitations of the study

One of the limitations of the current study is the use of a single syngeneic mouse model with different genetic backgrounds. We are aware that insights from one syngeneic mouse model may not fully recapitulate the EOC heterogeneity and may result in limited information for clinical translation outcomes. Additionally, we detected significant influence of IF on metabolic growth factors such as leptin, insulin, and IGF1, but we did not examine the mechanistic link between these growth factors on immunological responses, particularly IGF1. IGF1 is a well-known regulator of immune cell development, proliferation, differentiation, and metabolic activity of T cells and macrophages. More comprehensive independent studies are needed to link the physiologic alterations of fasting to fasting-induced anti-tumor immune responses.

STAR★METHODS

Detailed methods are provided in the online version of this paper and include the following:

- KEY RESOURCES TABLE
- RESOURCE AVAILABILITY
 - Lead contact
 - Materials availability
 - Data and code availability
- EXPERIMENTAL MODEL AND STUDY PARTICIPANT DETAILS
 - Cell lines and reagents
 - Animal model and experiments
- METHOD DETAILS
 - Fluorescence-activated cell sorting
 - ELISA
 - Adipokine array
 - Real-time PCR
 - Seahorse metabolic analysis
 - Ex-Vivo co-culture experiments
 - Metabolomics
 - Quantitation of BHB by LC-MS/MS
 - Sample preparation
 - Limit of detection (LOD) and lower limit of quantification (LLOQ)
 - Quantitative performance
 - BHB extraction and LC-MS/MS analysis
- QUANTIFICATION AND STATISTICAL ANALYSIS
- ADDITIONAL RESOURCES

SUPPLEMENTAL INFORMATION

Supplemental information can be found online at <https://doi.org/10.1016/j.isci.2023.107839w>.

ACKNOWLEDGMENTS

This work was supported by NIH/NCI R01CA249188 to RR. M.P.U and H.S. are partially supported by Henry Ford Cancer post-doctoral fellowship award. S.G. is supported by grants from the National Multiple Sclerosis Society (RG-1807-31964, RG-1508-05912), the NIH (NS112727, AI144004).

AUTHOR CONTRIBUTIONS

M.P.U., H.S., and N.T. performed research, analyzed the data, and edited the manuscript; F.R. and L.P. performed research and analyzed the data; I.D., M.H., M.S., A.M., and S.G. analyzed the data and edited the manuscript; R.R. designed and supervised research, analyzed the data, wrote, and edited the manuscript.

DECLARATION OF INTERESTS

The authors declare no competing interests.

INCLUSION AND DIVERSITY

We support, diverse and equitable conduction of research.

Received: May 9, 2023

Revised: June 28, 2023

Accepted: September 2, 2023

Published: September 9, 2023

REFERENCES

- Siegel, R.L., Miller, K.D., Wagle, N.S., and Jemal, A. (2023). Cancer statistics, 2023. *CA. Cancer J. Clin.* 73, 17–48. <https://doi.org/10.3322/caac.21763>.
- Bercow, A.S., Chen, L., Chatterjee, S., Tergas, A.I., Hou, J.Y., Burke, W.M., Ananth, C.V., Neugut, A.I., Hershman, D.L., and Wright, J.D. (2017). Cost of Care for the Initial Management of Ovarian Cancer. *Obstet. Gynecol.* 130, 1269–1275. <https://doi.org/10.1097/AOG.0000000000002317>.
- Suidan, R.S., He, W., Sun, C.C., Zhao, H., Rauh-Hain, J.A., Fleming, N.D., Lu, K.H., Giordano, S.H., and Meyer, L.A. (2019). Total and out-of-pocket costs of different primary management strategies in ovarian cancer. *Am. J. Obstet. Gynecol.* 221, 136.e1–136.e9. <https://doi.org/10.1016/j.ajog.2019.04.005>.
- Mittelman, S.D. (2020). The Role of Diet in Cancer Prevention and Chemotherapy Efficacy. *Annu. Rev. Nutr.* 40, 273–297. <https://doi.org/10.1146/annurev-nutr-013120-041149>.
- Zhang, F.F., Cudhea, F., Shan, Z., Michaud, D.S., Imamura, F., Eom, H., Ruan, M., Rehm, C.D., Liu, J., Du, M., et al. (2019). Preventable Cancer Burden Associated With Poor Diet in the United States. *JNCI Cancer Spectr.* 3, pkz034. <https://doi.org/10.1093/jncics/pkz034>.
- McCay, C.M., Crowell, M.F., and Maynard, L.A. (1989). The effect of retarded growth upon the length of life span and upon the ultimate body size. *Nutrition* 5, 155–171. [discussion 172](https://doi.org/10.1016/0022-3168(89)90007-7).
- Nencioni, A., Caffa, I., Cortellino, S., and Longo, V.D. (2018). Fasting and cancer: molecular mechanisms and clinical application. *Nat. Rev. Cancer* 18, 707–719. <https://doi.org/10.1038/s41568-018-0061-0>.
- Hursting, S.D., Lavigne, J.A., Berrigan, D., Perkins, S.N., and Barrett, J.C. (2003). Calorie restriction, aging, and cancer prevention: mechanisms of action and applicability to humans. *Annu. Rev. Med.* 54, 131–152. <https://doi.org/10.1146/annurev.med.54.101601.152156>.
- Vidoni, C., Ferraresi, A., Esposito, A., Maheshwari, C., Dhanasekaran, D.N., Mollace, V., and Isidoro, C. (2021). Calorie Restriction for Cancer Prevention and Therapy: Mechanisms, Expectations, and Efficacy. *J. Cancer Prev.* 26, 224–236. <https://doi.org/10.15430/JCP.2021.26.4.224>.
- Talib, W.H., Mahmood, A.I., Kamal, A., Rashid, H.M., Alashqar, A.M.D., Khater, S., Jamal, D., and Waly, M. (2021). Ketogenic Diet in Cancer Prevention and Therapy: Molecular Targets and Therapeutic Opportunities. *Curr. Issues Mol. Biol.* 43, 558–589. <https://doi.org/10.3390/cimb43020042>.
- Ferrere, G., Tidjani Alou, M., Liu, P., Goubet, A.G., Fidelle, M., Kepp, O., Durand, S., Iebba, V., Fluckiger, A., Daillère, R., et al. (2021). Ketogenic diet and ketone bodies enhance the anticancer effects of PD-1 blockade. *JCI Insight* 6, e145207. <https://doi.org/10.1172/jci.insight.145207>.
- Yang, L., TeSlaa, T., Ng, S., Nofal, M., Wang, L., Lan, T., Zeng, X., Cowan, A., McBride, M., Lu, W., et al. (2022). Ketogenic diet and chemotherapy combine to disrupt pancreatic cancer metabolism and growth. *Med (N Y)* 3, 119–136. <https://doi.org/10.1016/j.medj.2021.12.008>.
- de Cabo, R., and Mattson, M.P. (2019). Effects of Intermittent Fasting on Health, Aging, and Disease. *N. Engl. J. Med.* 381, 2541–2551. <https://doi.org/10.1056/NEJMra1905136>.
- Patterson, R.E., and Sears, D.D. (2017). Metabolic Effects of Intermittent Fasting. *Annu. Rev. Nutr.* 37, 371–393. <https://doi.org/10.1146/annurev-nutr-071816-064634>.
- Tang, X., Li, G., Shi, L., Su, F., Qian, M., Liu, Z., Meng, Y., Sun, S., Li, J., and Liu, B. (2021). Combined intermittent fasting and ERK inhibition enhance the anti-tumor effects of chemotherapy via the GSK3beta-SIRT7 axis. *Nat. Commun.* 12, 5058. <https://doi.org/10.1038/s41467-021-25274-3>.
- Bauersfeld, S.P., Kessler, C.S., Wischniewsky, M., Jaensch, A., Steckhan, N., Stange, R., Kunz, B., Brückner, B., Sehoul, J., and Michalsen, A. (2018). The effects of short-term fasting on quality of life and tolerance to chemotherapy in patients with breast and ovarian cancer: a randomized cross-over pilot study. *BMC Cancer* 18, 476. <https://doi.org/10.1186/s12885-018-4353-2>.
- Zorn, S., Ehret, J., Schäuble, R., Rautenberg, B., Ihorst, G., Bertz, H., Urbain, P., and Raynor, A. (2020). Impact of modified short-term fasting and its combination with a fasting supportive diet during chemotherapy on the incidence and severity of chemotherapy-induced toxicities in cancer patients - a controlled cross-over pilot study. *BMC Cancer* 20, 578. <https://doi.org/10.1186/s12885-020-07041-7>.
- Riedinger, C.J., Kimball, K.J., Kilgore, L.C., Bell, C.W., Heide, R.E., and Boone, J.D. (2020). Water only fasting and its effect on chemotherapy administration in gynecologic malignancies. *Gynecol. Oncol.* 159, 799–803. <https://doi.org/10.1016/j.ygyno.2020.09.008>.
- Vernieri, C., Fucà, G., Ligorio, F., Huber, V., Vingiani, A., Iannelli, F., Raimondi, A., Rinchai, D., Frigè, G., Belfiore, A., et al. (2022). Fasting-Mimicking Diet Is Safe and Reshapes Metabolism and Antitumor Immunity in Patients with Cancer. *Cancer Discov.* 12, 90–107. <https://doi.org/10.1158/2159-8290.CD-21-0030>.
- Pistollato, F., Forbes-Hernandez, T.Y., Iglesias, R.C., Ruiz, R., Elexpuru Zabaleta, M., Dominguez, I., Cianciosi, D., Quiles, J.L., Giampieri, F., and Battino, M. (2021). Effects of caloric restriction on immunosurveillance, microbiota and cancer cell phenotype: Possible implications for cancer treatment. *Semin. Cancer Biol.* 73, 45–57. <https://doi.org/10.1016/j.semcancer.2020.11.017>.
- Roby, K.F., Taylor, C.C., Sweetwood, J.P., Cheng, Y., Pace, J.L., Tawfik, O., Persons, D.L., Smith, P.G., and Terranova, P.F. (2000). Development of a syngeneic mouse model for events related to ovarian cancer. *Carcinogenesis* 21, 585–591. <https://doi.org/10.1093/carcin/21.4.585>.
- Walton, J., Blagih, J., Ennis, D., Leung, E., Dowson, S., Farquharson, M., Tookman, L.A., Orange, C., Athineos, D., Mason, S., et al. (2016). CRISPR/Cas9-Mediated Trp53 and Brca2 Knockout to Generate Improved Murine Models of Ovarian High-Grade Serous Carcinoma. *Cancer Res.* 76, 6118–6129. <https://doi.org/10.1158/0008-5472.CAN-16-1272>.
- Mandilaras, V., Garg, S., Cabanero, M., Tan, Q., Pastrello, C., Burnier, J., Karakasis, K., Wang, L., Dhani, N.C., Butler, M.O., et al. (2019). TP53 mutations in high grade serous ovarian cancer and impact on clinical outcomes: a comparison of next generation sequencing and bioinformatics analyses. *Int. J. Gynecol. Cancer* 29, 346–352. <https://doi.org/10.1136/ijgc-2018-000087>.
- Keller, U. (2019). Nutritional Laboratory Markers in Malnutrition. *J. Clin. Med.* 8, 775. <https://doi.org/10.3390/jcm8060775>.
- Weng, M.L., Chen, W.K., Chen, X.Y., Lu, H., Sun, Z.R., Yu, Q., Sun, P.F., Xu, Y.J., Zhu, M.M., Jiang, N., et al. (2020). Fasting inhibits aerobic glycolysis and proliferation in colorectal cancer via the Fdft1-mediated AKT/mTOR/HIF1alpha pathway suppression. *Nat. Commun.* 11, 1869. <https://doi.org/10.1038/s41467-020-15795-8>.
- de Groot, S., Pijl, H., van der Hoeven, J.J.M., and Kroep, J.R. (2019). Effects of short-term fasting on cancer treatment. *J. Exp. Clin. Cancer Res.* 38, 209. <https://doi.org/10.1186/s13046-019-1189-9>.
- Al-Wahab, Z., Tebbe, C., Chhina, J., Dar, S.A., Morris, R.T., Ali-Fehmi, R., Giri, S., Munkarah, A.R., and Rattan, R. (2014). Dietary energy balance modulates ovarian cancer progression and metastasis. *Oncotarget* 5, 6063–6075. <https://doi.org/10.18632/oncotarget.2168>.
- Harvey, A.E., Lashinger, L.M., Hays, D., Harrison, L.M., Lewis, K., Fischer, S.M., and Hursting, S.D. (2014). Calorie restriction decreases murine and human pancreatic tumor cell growth, nuclear factor-kappaB activation, and inflammation-related gene expression in an insulin-like growth factor-1-dependent manner. *PLoS One* 9, e94151.

- <https://doi.org/10.1371/journal.pone.0094151>.
29. Caffa, I., Spagnolo, V., Vernieri, C., Valdemarin, F., Becherini, P., Wei, M., Brandhorst, S., Zucal, C., Driehuis, E., Ferrando, L., et al. (2020). Fasting-mimicking diet and hormone therapy induce breast cancer regression. *Nature* 583, 620–624. <https://doi.org/10.1038/s41586-020-2502-7>.
 30. Qian, J., Fang, Y., Yuan, N., Gao, X., Lv, Y., Zhao, C., Zhang, S., Li, Q., Li, L., Xu, L., et al. (2021). Innate immune remodeling by short-term intensive fasting. *Aging Cell* 20, e13507. <https://doi.org/10.1111/ace1.13507>.
 31. Patel, C.H., and Powell, J.D. (2017). Targeting T cell metabolism to regulate T cell activation, differentiation and function in disease. *Curr. Opin. Immunol.* 46, 82–88. <https://doi.org/10.1016/j.coi.2017.04.006>.
 32. Buck, M.D., O'Sullivan, D., and Pearce, E.L. (2015). T cell metabolism drives immunity. *J. Exp. Med.* 212, 1345–1360. <https://doi.org/10.1084/jem.20151159>.
 33. Ho, P.C., Bihuniak, J.D., Macintyre, A.N., Staron, M., Liu, X., Amezquita, R., Tsui, Y.C., Cui, G., Micevic, G., Perales, J.C., et al. (2015). Phosphoenolpyruvate Is a Metabolic Checkpoint of Anti-tumor T Cell Responses. *Cell* 162, 1217–1228. <https://doi.org/10.1016/j.cell.2015.08.012>.
 34. van Bruggen, J.A.C., Martens, A.W.J., Fraietta, J.A., Hofland, T., Tonino, S.H., Eldering, E., Levin, M.D., Siska, P.J., Endstra, S., Rathmell, J.C., et al. (2019). Chronic lymphocytic leukemia cells impair mitochondrial fitness in CD8(+) T cells and impede CAR T-cell efficacy. *Blood* 134, 44–58. <https://doi.org/10.1182/blood.2018885863>.
 35. Cham, C.M., Driessens, G., O'Keefe, J.P., and Gajewski, T.F. (2008). Glucose deprivation inhibits multiple key gene expression events and effector functions in CD8+ T cells. *Eur. J. Immunol.* 38, 2438–2450. <https://doi.org/10.1002/eji.200838289>.
 36. Dar, S., Chhina, J., Mert, I., Chitale, D., Buekers, T., Kaur, H., Giri, S., Munkarah, A., and Rattan, R. (2017). Bioenergetic Adaptations in Chemoresistant Ovarian Cancer Cells. *Sci. Rep.* 7, 8760. <https://doi.org/10.1038/s41598-017-09206-0>.
 37. Pelleitier, M., and Montplaisir, S. (1975). The nude mouse: a model of deficient T-cell function. *Methods Achiev. Exp. Pathol.* 7, 149–166.
 38. Maiorano, B.A., Maiorano, M.F.P., Lorusso, D., and Maiello, E. (2021). Ovarian Cancer in the Era of Immune Checkpoint Inhibitors: State of the Art and Future Perspectives. *Cancers* 13, 4438. <https://doi.org/10.3390/cancers13174438>.
 39. Yang, C., Xia, B.R., Zhang, Z.C., Zhang, Y.J., Lou, G., and Jin, W.L. (2020). Immunotherapy for Ovarian Cancer: Adjuvant, Combination, and Neoadjuvant. *Front. Immunol.* 11, 577869. <https://doi.org/10.3389/fimmu.2020.577869>.
 40. Poisson, L.M., Munkarah, A., Madi, H., Datta, I., Hensley-Alford, S., Tebbe, C., Buekers, T., Giri, S., and Rattan, R. (2015). A metabolomic approach to identifying platinum resistance in ovarian cancer. *J. Ovarian Res.* 8, 13. <https://doi.org/10.1186/s13048-015-0140-8>.
 41. Udumula, M.P., Poisson, L.M., Dutta, I., Tiwari, N., Kim, S., Chhinna-Shankar, J., Allo, G., Sakr, S., Hijaz, M., Munkarah, A.R., et al. (2022). Divergent Metabolic Effects of Metformin Merge to Enhance Eicosapentaenoic Acid Metabolism and Inhibit Ovarian Cancer In Vivo. *Cancers* 14, 1504. <https://doi.org/10.3390/cancers14061504>.
 42. Puchalska, P., and Crawford, P.A. (2017). Multi-dimensional Roles of Ketone Bodies in Fuel Metabolism, Signaling, and Therapeutics. *Cell Metab.* 25, 262–284. <https://doi.org/10.1016/j.cmet.2016.12.022>.
 43. Taggart, A.K.P., Kero, J., Gan, X., Cai, T.Q., Cheng, K., Ippolito, M., Ren, N., Kaplan, R., Wu, K., Wu, T.J., et al. (2005). (D)-beta-Hydroxybutyrate inhibits adipocyte lipolysis via the nicotinic acid receptor PUMA-G. *J. Biol. Chem.* 280, 26649–26652. <https://doi.org/10.1074/jbc.C500213200>.
 44. Dmitrieva-Posocco, O., Wong, A.C., Lundgren, P., Golos, A.M., Descamps, H.C., Dohnalová, L., Cramer, Z., Tian, Y., Yueh, B., Eskioçak, O., et al. (2022). beta-Hydroxybutyrate suppresses colorectal cancer. *Nature* 605, 160–165. <https://doi.org/10.1038/s41586-022-04649-6>.
 45. Udumula, M.P., Sakr, S., Dar, S., Alvero, A.B., Ali-Fehmi, R., Abdulfatah, E., Li, J., Jiang, J., Tang, A., Buekers, T., et al. (2021). Ovarian cancer modulates the immunosuppressive function of CD11b(+)Gr1(+) myeloid cells via glutamine metabolism. *Mol. Metab.* 53, 101272. <https://doi.org/10.1016/j.molmet.2021.101272>.
 46. Buono, R., and Longo, V.D. (2018). Starvation, Stress Resistance, and Cancer. *Trends Endocrinol. Metab.* 29, 271–280. <https://doi.org/10.1016/j.tem.2018.01.008>.
 47. Lee, C., Raffaghella, L., Brandhorst, S., Safdie, F.M., Bianchi, G., Martin-Montalvo, A., Pistoia, V., Wei, M., Hwang, S., Merlino, A., et al. (2012). Fasting cycles retard growth of tumors and sensitize a range of cancer cell types to chemotherapy. *Sci. Transl. Med.* 4, 124ra27. <https://doi.org/10.1126/scitranslmed.3003293>.
 48. Han, Y.M., Ramprasath, T., and Zou, M.H. (2020). beta-hydroxybutyrate and its metabolic effects on age-associated pathology. *Exp. Mol. Med.* 52, 548–555. <https://doi.org/10.1038/s12276-020-0415-z>.
 49. Newman, J.C., Covarrubias, A.J., Zhao, M., Yu, X., Gut, P., Ng, C.P., Huang, Y., Haldar, S., and Verdin, E. (2017). Ketogenic Diet Reduces Midlife Mortality and Improves Memory in Aging Mice. *Cell Metab.* 26, 547–557.e8. <https://doi.org/10.1016/j.cmet.2017.08.004>.
 50. Mikami, D., Kobayashi, M., Uwada, J., Yazawa, T., Kamiyama, K., Nishimori, K., Nishikawa, Y., Nishikawa, S., Yokoi, S., Taniguchi, T., and Iwano, M. (2020). beta-Hydroxybutyrate enhances the cytotoxic effect of cisplatin via the inhibition of HDAC/survivin axis in human hepatocellular carcinoma cells. *J. Pharmacol. Sci.* 142, 1–8. <https://doi.org/10.1016/j.jpshs.2019.10.007>.
 51. Shukla, S.K., Gebregiorgis, T., Purohit, V., Chaika, N.V., Gunda, V., Radhakrishnan, P., Mehla, K., Pipinos, I.I., Powers, R., Yu, F., and Singh, P.K. (2014). Metabolic reprogramming induced by ketone bodies diminishes pancreatic cancer cachexia. *Cancer Metab.* 2, 18. <https://doi.org/10.1186/2049-3002-2-18>.
 52. Poff, A.M., Ari, C., Arnold, P., Seyfried, T.N., and D'Agostino, D.P. (2014). Ketone supplementation decreases tumor cell viability and prolongs survival of mice with metastatic cancer. *Int. J. Cancer* 135, 1711–1720. <https://doi.org/10.1002/ijc.28809>.
 53. Skinner, R., Trujillo, A., Ma, X., and Beierle, E.A. (2009). Ketone bodies inhibit the viability of human neuroblastoma cells. *J. Pediatr. Surg.* 44, 212–216. discussion 216. <https://doi.org/10.1016/j.jpedsurg.2008.10.042>.
 54. Rodrigues, L.M., Uribe-Lewis, S., Madhu, B., Honess, D.J., Stubbs, M., and Griffiths, J.R. (2017). The action of beta-hydroxybutyrate on the growth, metabolism and global histone H3 acetylation of spontaneous mouse mammary tumours: evidence of a beta-hydroxybutyrate paradox. *Cancer Metab.* 5, 4. <https://doi.org/10.1186/s40170-017-0166-z>.
 55. Gouirand, V., Gicquel, T., Lien, E.C., Jaune-Pons, E., Da Costa, Q., Finetti, P., Metay, E., Duluc, C., Mayers, J.R., Audebert, S., et al. (2022). Ketogenic HMG-CoA lyase and its product beta-hydroxybutyrate promote pancreatic cancer progression. *EMBO J.* 41, e110466. <https://doi.org/10.15252/emboj.2021110466>.
 56. Ghahremani, H., Nabati, S., Tahmori, H., Peirouvi, T., Sirati-Sabet, M., and Salami, S. (2021). Long-Term Glucose Restriction with or without beta-Hydroxybutyrate Enrichment Distinctly Alters Epithelial-Mesenchymal Transition-Related Signalings in Ovarian Cancer Cells. *Nutr. Cancer* 73, 1708–1726. <https://doi.org/10.1080/01635581.2020.1804947>.
 57. Cohen, C.W., Fontaine, K.R., Arend, R.C., Alvarez, R.D., Leath, C.A., III, Huh, W.K., Bevis, K.S., Kim, K.H., Straughn, J.M., Jr., and Gower, B.A. (2018). A Ketogenic Diet Reduces Central Obesity and Serum Insulin in Women with Ovarian or Endometrial Cancer. *J. Nutr.* 148, 1253–1260. <https://doi.org/10.1093/jn/nxy119>.
 58. Cohen, C.W., Fontaine, K.R., Arend, R.C., and Gower, B.A. (2020). A Ketogenic Diet Is Acceptable in Women with Ovarian and Endometrial Cancer and Has No Adverse Effects on Blood Lipids: A Randomized, Controlled Trial. *Nutr. Cancer* 72, 584–594. <https://doi.org/10.1080/01635581.2019.1645864>.
 59. Hirschberger, S., Strauß, G., Effinger, D., Marstaller, X., Ferstl, A., Müller, M.B., Wu, T., Hübner, M., Rahmel, T., Mascolo, H., et al. (2021). Very-low-carbohydrate diet enhances human T-cell immunity through immunometabolic reprogramming. *EMBO Mol. Med.* 13, e14323. <https://doi.org/10.15252/emmm.202114323>.
 60. Zander, R., Schauder, D., Xin, G., Nguyen, C., Wu, X., Zajac, A., and Cui, W. (2019). CD4(+) T Cell Help Is Required for the Formation of a Cytolytic CD8(+) T Cell Subset that Protects against Chronic Infection and Cancer. *Immunity* 51, 1028–1042.e4. <https://doi.org/10.1016/j.immuni.2019.10.009>.
 61. Maifeld, A., Bartolomaeus, H., Löber, U., Avery, E.G., Steckhan, N., Markó, L., Wilck, N., Hamad, I., Sušnjär, U., Mähler, A., et al.

- (2021). Fasting alters the gut microbiome reducing blood pressure and body weight in metabolic syndrome patients. *Nat. Commun.* 12, 1970. <https://doi.org/10.1038/s41467-021-22097-0>.
62. Zhang, L., Yang, N., Garcia, J.R.C., Mohamed, A., Benencia, F., Rubin, S.C., Allman, D., and Coukos, G. (2002). Generation of a syngeneic mouse model to study the effects of vascular endothelial growth factor in ovarian carcinoma. *Am. J. Pathol.* 161, 2295–2309. [https://doi.org/10.1016/s0002-9440\(10\)64505-1](https://doi.org/10.1016/s0002-9440(10)64505-1).
63. Meng, X., Wang, Y., and Zhu, L. (2018). [Automatic clustering method of flow cytometry data based on t-distributed stochastic neighbor embedding]. *Sheng Wu Yi Xue Gong Cheng Xue Za Zhi* 35, 697–704. <https://doi.org/10.7507/1001-5515.201802037>.
64. Fehlings, M., Simoni, Y., Penny, H.L., Becht, E., Loh, C.Y., Gubin, M.M., Ward, J.P., Wong, S.C., Schreiber, R.D., and Newell, E.W. (2017). Checkpoint blockade immunotherapy reshapes the high-dimensional phenotypic heterogeneity of murine intratumoural neoantigen-specific CD8(+) T cells. *Nat. Commun.* 8, 562. <https://doi.org/10.1038/s41467-017-00627-z>.
65. Zhou, L., Ruan, M., Liu, Y., Zhu, Y., Fu, D., Wu, K., and Zhang, Q. (2020). B7H4 expression in tumor cells impairs CD8 T cell responses and tumor immunity. *Cancer Immunol. Immunother.* 69, 163–174. <https://doi.org/10.1007/s00262-019-02451-4>.
66. Zahoor, I., Suhail, H., Datta, I., Ahmed, M.E., Poisson, L.M., Waters, J., Rashid, F., Bin, R., Singh, J., Cerghet, M., et al. (2022). Blood-based untargeted metabolomics in relapsing-remitting multiple sclerosis revealed the testable therapeutic target. *Proc. Natl. Acad. Sci. USA* 119, e2123265119. <https://doi.org/10.1073/pnas.2123265119>.

STAR★METHODS

KEY RESOURCES TABLE

REAGENT or RESOURCE	SOURCE	IDENTIFIER		
Antibodies				
<i>InVivoMab</i> anti-mouse PD-1	BioXCell	Cat#BE0146; RRID:AB_10949053.		
<i>InVivoMab</i> rat IgG2b isotype	BioXCell	Cat#BE0090; RRID:AB_1107780		
<i>InVivoMab</i> anti-mouse CD4	BioXCell	Cat#BP0003; RRID:AB_1107636		
<i>InVivoMab</i> anti-mouse CD8 α	BioXCell	Cat#BE0061; RRID:AB_1125541		
Chemicals, peptides, and recombinant proteins				
Oligomycin	Cayman Chemical	Cat#11342		
FCCP	Cayman Chemical	Cat#15218		
Antimycin-A	Cayman Chemical	Cat#19433		
Rotenone	Cayman Chemical	Cat#13995		
2-Deoxyglucose (2DG)	Cayman Chemical	Cat#17149		
B-Hydroxy butyric acid	Sigma Aldrich	Cat#H6501		
D-3-hydroxybutyrate	Cambridge Isotope Laboratories	Cat#CLM-3853-0.5		
Critical commercial assays				
Pre-albumin	Crystal Chem Inc	Cat#80732		
BHB	Cayman Chemical	Cat#700190		
Adipokine array	R&D systems	Cat#ARY013		
Softwares				
GraphPad Prism 8		GraphPad Software		
T-Distributed Stochastic Neighbor Embedding (tSNE)		Flowjo software (Version 10.8.1)		
Experimental models: Cell lines				
ID8 ^{p53+/+}	Laboratory of McNeish	N/A		
ID8 ^{p53-/-}	Laboratory of McNeish	N/A		
ID8 ^{p53-/-, PTEN-/-}	Laboratory of McNeish	N/A		
Experimental models: Organisms/strains				
Mouse: C57/B6	The Jackson Laboratory	JAX: 000664; RRID:IMSR_JAX:000664		
Oligonucleotides				
BDH 1	Integrated DNA technology (ITD)	Fw: GAA AGT GGT GGA GAT TGT CCG C Rv: TGT AGG TCT CCA GGC TGG TGA A		
GPR 109a	Integrated DNA technology (ITD)	Fw: CGAGGTGGCTGAGGCTGGAATTGGGT Rv: ATTTGCAGGGCCATTCTGGAT		
ACAT	Integrated DNA technology (ITD)	Fw: TGA GAG CAC CTC CAG AAC AAG G Rv: GGA CGA ATA GGA TGA GGA GTG C		
HMGCS2	Integrated DNA technology (ITD)	Fw: CCT TGA ACG AGT GGA TGA GA Rv: CAG ATG CTG TTT GGG TAG CA		
HMGCL	Integrated DNA technology (ITD)	Fw: ACCACCAGCTTTGTGTCTCC Rv: GAGGCAGCTCCAAAGATGAC		
L27	Integrated DNA technology (ITD)	Fw: ACA TTG ACG ATG GCA CCT C Rv: GCT TGG CGA TCT TCT TCT TG		
FACS Fluorochromes				
Antibody	Clone	Fluorochrome	Source	Identifier
CD3	17A2	AF700	Biologend	Cat#100202; RRID:AB_312659

(Continued on next page)

Continued

REAGENT or RESOURCE	SOURCE		IDENTIFIER	
Granzyme B	QA16A02	PE-CY5	Biolegend	Cat#372226; RRID:AB_2943488
Perforin	S16009A	PE	Biolegend	Cat#154306; RRID:AB_2721639
CD4	GK.1.5	BV510	Biolegend	Cat#154306; RRID:AB_2721639
IFN γ	XMG1.2	PE/Dazzle 594	Biolegend	Cat#505846; RRID:AB_2563980
IL4	11B11	PE-CY7	Biolegend	Cat#504118; RRID:AB_10898116
CD8	53-6.7	Percp-CY5.5	Biolegend	Cat#100734; RRID:AB_2075238
CD45	S18009F	FITC	Biolegend	Cat#157214; RRID:AB_2943492

RESOURCE AVAILABILITY

Lead contact

Further information and requests for resources and reagents should be directed to and will be fulfilled by the lead contact, Ramandeep Rattan (rrattan1@hfhs.org).

Materials availability

The study did not generate any new unique reagents.

Data and code availability

- This paper does not analyze any publicly available data.
- All data reported in the paper will be shared by the [lead contact](#) upon request.
- This paper does not report original code.
- Any additional information required to reanalyze the reported data is available from the [lead contact](#) upon request.

EXPERIMENTAL MODEL AND STUDY PARTICIPANT DETAILS

Cell lines and reagents

ID8^{p53+/+}, TRP53 mutated (ID8^{p53-/-}) and PTEN mutated (ID8^{p53-/-}, PTEN^{-/-}) ID8 cells were a gift from Dr. Ian McNeish (Imperial College, London).²² All the cell lines were cultured in Dulbecco's modified Eagles media (Hyclone, Logan, UT), 5% FBS (BioAbChem, Ladson, SC), 4% Insulin -Transferrin-Selenium (Invitrogen), 100 U/ml penicillin and 100 U/ml streptomycin (Hyclone, Logan, UT), 2 mM L-glutamine, 1 mM sodium pyruvate. All cells were cultured at 37°C in a humidified 5% CO₂ incubator. DL- β hydroxybutyric (BHB) acid sodium salt was purchased from Sigma-Aldrich (Burlington, MA).

Animal model and experiments

Induction of intra-peritoneal ovarian tumor

C57/B6 female mice of 6–8 weeks were acquired from Jackson Laboratory (Bar Harbor, ME) and were maintained under standard optimized conditions in the animal facility at Henry Ford Hospital (Detroit, MI). Prior to the start of the study, mice were acclimated in house for one week. To induce ovarian cancer, mice were injected intraperitoneally (IP) with 10×10^6 ID8 cells (ID8^{p53+/+} or ID8^{p53-/-} or ID8^{p53-/-} PTEN^{-/-}) in 200 μ L of PBS. After one week of tumor induction mice were randomly divided into regular diet (RD) or intermittent fasting (IF) groups. Monitoring for tumor burden was performed by tracking weight, abdominal circumference, and ascites formation.^{27,45} Mice that experienced severe signs of clinical distress (cachexia, anorexia, increased respiration, excess ascites) or when abdominal circumference exceeded 8 cm, or impaired mobility or bodily functions, were immediately euthanized.

Induction of subcutaneous ovarian tumor

Subcutaneous ovarian tumors were initiated by injecting 2×10^6 ID8^{p53-/-} cells suspended in 150 μ L of 50% Matrigel (Corning Life Science, Massachusetts) in the subcutaneous layer of the left flank of the mice. Once visible, the tumors were measured using a digital Vernier caliper. Tumor volume was calculated by using the standard formula $1/2(L \times W)^2$, where L is the longest and W is the shorter length measured.⁶² After the formation of visible tumors, tumor volume was assessed weekly.

Intermittent fasting protocol

IF intervention consisted of 16 h of fasting and 8 h of *ad libitum* feeding for five consecutive days and two consecutive days of 24-h *ad libitum* feeding during the week. The regular diet (RD) control group received 24 h, 7 days a week *ad libitum* feeding throughout the study.

Continuous access to water was provided to all mice throughout the study. IF was initiated one week after tumor injections and mice were monitored every other day till the end of the study. Food intake was measured over a period of one week at multiple time points during the study.

Treatments

All treatments were started after one week of tumor injection and each treatment group consisted of 10 mice. Immunotherapy groups received *InVivoMab* anti-mouse PD-1 or control *InVivoMab* rat IgG2b isotype given IP once a week at 100 μ g/mice for 4 weeks alone or in combination with IF. In depletion experiments, mice were treated with *InVivoMab* anti-mouse CD8 α (200 μ g/mice) or *InVivoPlus* anti-mouse CD4 (200 μ g/mice) or *InVivoMab* rat IgG2b (BioXcell, Lebanon, NH) twice via IP injections per week for a total of 6 doses. Depletion efficacy was measured by flow cytometry after 4 doses of antibody injections. All antibodies ([key resources table](#)) were purchased from BioXcell (West Lebanon, NH). BHB treatments were given IP at the dose of 300 mg/kg bd wt thrice weekly, while the control mice received PBS.

Survival curve

For estimating overall survival, $n = 12$ mice per group were injected with respective ID8 cells and tumors were allowed to proceed until the abdominal circumference reached 8 cm, according to the Hospital Institutional Animal Care and Use Committee (IACUC) approved endpoint. The mice were then humanely euthanized. Survival curves were generated using Kaplan-Meier analysis using Prism 8 (GraphPad Software, La Jolla, CA).

Ethics statement

All protocols were approved by the Henry Ford Hospital IACUC prior to any experiments. All institutional and national guidelines for the care and use of laboratory animals were followed. Only female mice were used to model EOC.

METHOD DETAILS

Fluorescence-activated cell sorting

Surface staining (CD45, CD3, CD4, CD8) and intracellular staining (IFN- γ , IL4, Granzyme B and Perforin) was performed in ascites and blood according to manufacturer's recommended dilution and as published before.⁴⁵ Surface marker antibodies were exposed for 30 min at 4°C. To analyze intracellular markers like IFN- γ , IL4, Granzyme B and Perforin, lymphocytes were treated for 5 h with GolgiPlug (BD Biosciences, San Jose, CA) followed by surface staining with antibodies against CD4 or CD8. Cells were washed, fixed, and permeabilized with cytofix/cytoperm buffer (Proteintech, Rosemont, IL, USA) followed by incubation with various antibodies against intracellular markers. Flow cytometric analysis was performed on a BD FACS Calibur (BD Biosciences, San Jose, CA, USA), and results were analyzed using Flowjo software (Version 10.8.1; BD Biosciences, San Jose, CA, USA). T-Distributed Stochastic Neighbor Embedding (tSNE) clusters were prepared using Flowjo software (Version 10.8.1).^{63,64} All fluorochrome labeled antibodies ([key resources table](#)) were purchased from Biolegend (San Diego, CA, USA).

ELISA

The levels of IL-6, IL-1 β , IL-4, IL-10, IFN γ , MCP-1, TNF α (Biolegend, San Diego, CA, USA), GM-CSF, IGF-1, Leptin, Adiponectin, Insulin (R&D Biosystems Minneapolis, MN, USA), Pre-albumin (Crystal Chem Inc., El Grove Village, IL, USA), and BHB (Cayman Chemical, Ann Arbor, MI, USA) in ascites, plasma or cell culture supernatants were measured according to manufacturers' instructions.⁴⁵ ELISA kits are listed in [Table S2](#).

Adipokine array

Ascites collected from RD and IF mice ($n = 4$ /group) were pooled and diluted 1:3 and applied in the adipokine array (ARY-013, R&D systems, Minneapolis, MN, USA). The proteome profiler adipokine array detects 38 adipokines ([Table S1](#)) in duplicate on nitrocellulose membranes. Expression of the adipokines were analyzed by Quick spots software designed for proteome arrays (R&D Systems, Minneapolis, MN, USA).

Real-time PCR

RNA was extracted (Qiagen, Valencia, CA, USA) and quantified (Qubit Fluorometer, Invitrogen, Waltham, MA, USA) from liver, and purified CD4⁺ and CD8⁺ T-cells prior to quantifying mRNA expression by Qubit Fluorometer (Invitrogen, Waltham, MA).⁴⁵ Reverse transcription was performed using 1 μ g of total RNA using high-capacity cDNA kit in 20- μ L reaction mixture and real-time polymerase chain reactions were performed and quantified as previously described⁴⁵ using CFX Bio-Rad Laboratories Real-time PCR Detection system (Hercules, CA). Ribosomal protein L27 was used as a housekeeping gene. All primers were purchased from Integrated DNA Technologies (Coralville, IA). Primer (Integrated DNA Technologies, Coralville, IA) sequences for acetyl coenzyme A acetyltransferase (ACAT), 3-Hydroxy-3-methylglutaryl-CoA synthase (HMGCS2), 3-Hydroxy-3-methylglutaryl-CoA lyase (HMGCL), beta-hydroxybutyrate dehydrogenase 1 (BDH1), Succinyl-CoA:3-ke-toacid CoA transferase (SCOT) and G protein-coupled receptor 109a (GPR109a, also known as Hydroxycarboxylic acid receptor 2, HCA₂) are listed in [key resources table](#).

Seahorse metabolic analysis

CD4⁺ and CD8⁺ cells were isolated from spleens of RD and IF tumor bearing mice using BD-IMAG anti-mouse CD4 and CD8 magnetic particles (BD Biosciences, San Jose, CA) and were plated at a density of 7×10^5 cells/well in cell-tak coated XFe 96 cell plates. Oxygen consumption rate (OCR) and Extracellular acidification (ECAR) rate were measured using XFe 96 seahorse analyzer (Agilent, Santa Clara, CA, USA) and analyzed as described.^{36,45} OCR measurements were recorded with port injections of (1) oligomycin (1 μ mol), (2) FCCP (0.5 μ mol), and a combination of (3) rotenone-antimycin at 1 μ mol. ECAR, an indicator of aerobic glycolysis, was measured by incubating cells in an XFe base medium supplemented with 2 mmol/L glutamine. ECAR measurements were recorded after injecting with (1) glucose (10 mM), followed by (2) oligomycin (2 μ M), and (3) 2-DG (100 mM). All media and coated plates were purchased from Agilent Technologies (Santa Clara, CA).

Ex-Vivo co-culture experiments

CD8⁺ and CD4⁺ T-cells isolated from spleens of naive mice using BD-IMAG anti-mouse CD4⁺ and CD8⁺ magnetic particles (BD Biosciences, San Jose, CA, USA) were cultured in 96-well plates (Nunc, Wiesbaden, Germany) at a density of 3×10^5 cells/well in 200 μ L RPMI 1640, supplemented with 5% serum, 100 U/mL penicillin, 100 μ g/mL streptomycin, 2 mM L-glutamine, and 1 mM sodium pyruvate. The cells were activated for 72 h in presence of recombinant mouse IL-2 (10 ng/mL) (BD Pharmingen Biosciences, San Diego, CA, USA) and Gibco Dyna mouse CD3/CD28 beads (Thermo Fischer, Detroit, MI, USA). One set was treated with 10 mM BHB, and after 72 h, 7AAD (eBioscience, San Diego, CA, USA) labeled 3×10^5 ID8^{p53-/-} tumor cells/well were added to the plates for another 72 h. Flow cytometry was performed to enumerate 7AAD⁺ tumor cells and the unlabeled T cells.⁶⁵ IFN γ release in the cell supernatant was determined by ELISA after 48 h of co-culture.

Metabolomics

Metabolomic profiling was performed by Metabolon Inc. (Morrisville, MA, USA). Statistical and bioinformatic analysis was performed by the Bioinformatics core at HFH as previously described.^{40,41,66}

Quantitation of BHB by LC-MS/MS

The levels of BHB in ascites and plasma of untreated, BHB treated and IF mice were quantified by ultrahigh performance liquid chromatography-tandem mass spectroscopy (UPLC-MS/MS) (Waters, Milford, MA, USA).⁶⁶ *Chemicals and reagents:* β -Hydroxybutyric acid standard was purchased from Sigma Aldrich (St Louis, MO) and isotopically labeled D-3-hydroxybutyrate (¹³C4) used as an internal standard (ISTD), were purchased from Cambridge Isotope Laboratories (Tewksbury, MA). Acetonitrile, Water and Methanol and Formic acid, were purchased from Sigma Aldrich (St Louis, MO).

Sample preparation

Concentrated stock solutions of β -Hydroxybutyric acid (β -HBA) standard (10 μ g/mL) and the ISTD (250 μ g/mL) were prepared in a 1:1 water: acetonitrile solution. Working solutions were prepared in matrix ranged from 15.75 to 1000 ng/mL for β -HBA. An ISTD working solution (0.500 ng/mL) was prepared in the extraction solvent 1:1 Water: acetonitrile. Calibration curve standards were prepared in duplicate for absolute concentration, while QC and blank (non-spiked) samples were prepared in Triplicates.

Limit of detection (LOD) and lower limit of quantification (LLOQ)

Seven calibration standards ranging from (15.75, 31.25, 62.5, 125, 250, 500 and 1000 ng/ml) 15.75–1000 ng/ml was subjected to the full extraction procedure three times before analysis. The limit of detection (LOD) was defined as the β -HBA concentration corresponding to the lowest calibration point, where signal to noise ratio (*s/n*) was three times greater than from the blank signal and lower limit of quantification was signal 10 times more compared to *s/n* with blank. *Data analysis:* Mass spectrometric data was acquired by MassLynx v4.2 software. Quantification software: TargetLynx software was used for preparing the calibration curve and absolute quantitation of β -HBA in the samples. Analyte concentrations were calculated using a 1/*x* weighted linear regression analysis of the standard curve.

Quantitative performance

The quantitative performance using this sample preparation and LC-MS method was excellent, achieving an LLOQ of 15.75 ng/mL for β -HBA. Calibration curves were linear ($r^2 > 0.996$) from 15.75 to 1000 ng/mL with accuracies between 85 and 115% with CVs.

BHB extraction and LC-MS/MS analysis

Experiment was setup for extraction and analysis conditions were optimized with RD, IF, control, β -BHA treatments. β -BHA absolute quantitation was performed in plasma and ascites. 100 μ L of plasma and ascites was used for extraction of the desired molecules using an in-house method for both the matrices. 300 μ L of acetonitrile was added to 100 μ L plasma and Ascites for protein precipitation and extraction of target molecule followed by 15 min of centrifugation at 15,000 rpm at 40°C. 350 μ L of upper layer was collated into fresh tube for complete drying under N₂ based evaporation at room temperature. The dried residue was re-suspended in 500 μ L diluent (Waters: Acetonitrile), vortexed and centrifuged (15 min at 15,000 g at 4°C), and placed in an auto sampler vial for LC-MS/MS analysis. Waters UPLC-TQD mass spectrometry was employed for method development including the LC method optimization, ionization, and fragmentation tests. The binary pump was used to

transport mobile phase A (Water+0.2% formic acid) and B (Acetonitrile+0.2% formic acid) at a flow rate of 0.3 mL/min in gradient mode. Best separation of β -Hydroxybutyric acid was achieved using UPLC with auto sampler with reversed-phase waters Atlantis dC18 Column, 130 Å, 3 μ m, 2.1 mm \times 100 mm (P/N: 186001295) with in-line filter and guard kept at 50°C. A 5 min gradient employed an initial condition of 90% A with linear gradient to 60% A at 2.00 min, followed by linear gradient to 40% A at 3.50 min, followed by a return to 90% A in 0.3 min with 1.2 min re-equilibration with initial condition for β -Hydroxybutyric acid separation. The auto sampler was maintained at 4°C to compound stable and the injection volume was 5 μ L with total running time of 5 min.

QUANTIFICATION AND STATISTICAL ANALYSIS

An unpaired Student's *t* test or one-way ANOVA was used where appropriate. Kaplan Meier analysis was used to determine the survival curve. The significance of survival curves was estimated by using the Gehan Breslow-Wilcoxon test. All analyses were carried out using Prism 8 (GraphPad Software, La Jolla, CA).

ADDITIONAL RESOURCES

This study does not involve any Clinical Trial.